

A SLIDING MODE CONTROLLER FOR INDUCTION MOTOR DRIVES

*A thesis submitted to National Institute of Technology, Rourkela,
for the award of the degree of*

Master of Technology

In

ELECTRICAL ENGINEERING

(Power Control and Drives)

by

PRAGYANSHREE PARIDA



DEPARTMENT OF ELECTRICAL ENGINEERING
NATIONAL INSTITUTE OF TECHNOLOGY
ROURKELA-769008, ORISSA
MAY, 2009

A SLIDING MODE CONTROLLER FOR INDUCTION MOTOR DRIVES

*A thesis submitted to National Institute of Technology, Rourkela,
for the award of the degree of*

Master of Technology

In

**ELECTRICAL ENGINEERING
(Power Control and Drives)**

by

PRAGYANSHREE PARIDA

Under the guidance of

Prof. K. B. Mohanty



**DEPARTMENT OF ELECTRICAL ENGINEERING
NATIONAL INSTITUTE OF TECHNOLOGY
ROURKELA-769008, ORISSA
MAY, 2009**

CERTIFICATE

This is to certify that the work in this thesis entitled “**A SLIDING MODE CONTROLLER FOR INDUCTION MOTOR DRIVES**” submitted by **Ms. PRAGYANSHREE PARIDA**, has been carried out under my supervision in partial fulfillment of the requirements for the degree of Master of Technology in ‘*Power Control and Drives*’ during session 2008-2009 in the Department of Electrical Engineering, National Institute of Technology, Rourkela (Deemed university) and is an authentic work by her under my supervision and guidance.

To the best of my knowledge and belief, this work has not been submitted to any other university or institution for the award of any degree or diploma.

Place:

Prof. K.B.Mohanty

Dept. of Electrical Engineering
National Institute of Technology,
Rourkela – 769008, Orissa

ACKNOWLEDGEMENTS

On the submission of my Thesis report of “**A Sliding Mode Controller for Induction Motor Drives**”, I wish to express my deep sense of gratitude to my supervisor **Dr. K. B. Mohanty**, Asst. Professor, Department of Electrical Engineering for his constant motivation and support during the course of my work in the last one year. I truly appreciate and value his esteemed guidance and encouragement from the beginning to the end of this thesis. His knowledge and company at the time of crisis would be remembered lifelong.

I am grateful to Prof. B.D. Subuddhi, present head of the Department and Prof. S. Ghosh, ex-Head of the Department for extending me all the possible facilities to carry out the research work.

I want to thank all my teachers for providing a solid background for my studies and research thereafter. They have been great sources of inspiration to me and I thank them from the bottom of my heart.

I will be failing in my duty if I do not mention the laboratory staff and administrative staff of this department for their timely help.

I would like to thank all whose direct and indirect support helped me completing my thesis in time.

Date:

Place: NIT, Rourkela

Pragyanshree Parida

MTech (Power Control and Drives)

ABSTRACT

Induction motors are being applied today to a wider range of applications requiring variable speed. Generally, variable speed drives for Induction Motor require both wide operating range of speed and fast torque response, regardless of any disturbances and uncertainties (like load variation, parameters variation and un-modeled dynamics). This leads to more advanced control methods to meet the real demand. The recent advances in the area of field-oriented control along with the rapid development and cost reduction of power electronics devices and microprocessors have made variable speed induction motor drives an economical alternative for many industrial applications. These AC drives are nowadays replacing their DC counter part and are becoming a major component in today's sophisticated industrial manufacturing and process automation. Advent of high switching frequency PWM inverters has made it possible to apply sophisticated control strategies to AC motor drives operating from variable voltage, variable frequency source. The complexity in there mathematical model and the consequent need for the sophisticated algorithms are being handled by the computational power of low cost microprocessors to digital signal processors (DSPs).

In the formulation of any control problem there will typically be discrepancies between the actual plant and the mathematical model developed for controller design. This mismatch may be due to un-modeled dynamics, variation in system parameters or the approximation of complex plant behavior by a straightforward model. The designer must ensure that the resulting controller has the ability to produce required performance levels in practice despite such plant/model mismatches. This has led to an intense interest in the development of robust control methods which seek to solve this problem. One particular approach to robust-control controller design is the so-called sliding mode control methodology.

In this dissertation report, a sliding mode controller is designed for an induction motor drive. The gain and band width of the controller is designed considering rotor resistance variation, model in accuracies and load disturbance, to have an ideal speed tracking. The chattering effect is also taken into account. The controller is simulated under various conditions and a comparative study of the results with that of PI controller has been presented.

TABLE OF CONTENTS

ABSTRACT	i
TABLE OF CONTENTS	ii
LIST OF SYMBOLS	iv
LIST OF FIGURES	vi
1. INTRODUCTION	1
1.1 Introduction	1
1.1.1 Scalar control	1
1.1.2 Vector control	2
1.2 Flux observer and speed estimation	3
1.3 Necessity of a robust controller	5
1.4 Sliding mode controller	6
1.5 Organization of the thesis	7
2. MODELLING OF INDUCTION MOTOR	9
2.1 Introduction	9
2.2 Induction motor model	9
2.3 The field oriented control	13
2.4 Estimation of speed	14
2.5 Chapter conclusion	17
3. DESIGN OF A SLIDING MODE CONTROLLER	18
3.1 Introduction	18
3.2 Sliding mode controller	19
3.2.1 Derivation of control law	24
3.2.2 Design of controller gain	24
3.2.3 Reduction of chattering	25
3.2.4 Design of band width, λ	26
3.3 Chapter conclusion	28

4. SIMULATION RESULTS AND DISCUSSIONS	29
5. CONCLUSION AND FUTURE WORK	43
REFERENCES	44
APPENDIX-A	47

LIST OF SYMBOLS

d	Disturbance or noise in the sliding mode controller
E	Error vector in sliding mode controller
e	Error in a state (say, speed)
f	Supply frequency in Hz
G	A function in sliding mode controller which is estimated
i_a, i_b, i_c	Stator phase (a, b, c) currents
J	Polar moment of inertia of the motor
K	Gain of sliding mode controller
K_{max}	Maximum gain of the sliding mode controller
K_p, K_i	Proportional gain and integral gain of the P-I controller
K_t	Torque constant of the motor
L_s, L_r	Self inductance per phase of stator and rotor referred to stator
L_m	Magnetizing inductance per phase referred to stator
l_s, l_r	Leakage inductance per phase of stator and rotor referred to stator
P	No. of pole pairs
R_s, R_r	Resistance per phase of stator and rotor referred to stator
S	Sliding surface
s	Distance of a state (say speed) from the sliding surface
T_e	Electromagnetic torque developed by the motor
T_l	Load torque
u	Input control voltage vector
V_a^*, V_b^*, V_c^*	Reference voltage for a-b-c phase of the inverter
V_{dc}	DC link voltage
V_m	Peak of the supply voltage per phase
V_{ab}, V_{bc}	Line to line voltage of the motor
V_{ds}, V_{qs}	d- and q-axis stator voltages
X	State vector
y	Out put vector

ω_r	Rotor mechanical speed (rad/sec)
ω_r^*	Reference/set speed (rad/sec)
ω_e	Speed of the reference frame (rad/sec)
ω_{sl}	Electrical slip speed (rad/sec)
ψ_{dr}, ψ_{qr}	d-axis and q-axis rotor flux linkages
$\psi_{\alpha r}, \psi_{\beta r}$	Components of rotor flux linkage vector in stationary (α - β) reference frame
$\psi_{\alpha s}, \psi_{\beta s}$	Components of stator flux linkage vector in stationary (α - β) reference frame
λ	Band width of the sliding mode controller
ϕ	Width of the boundary layer for the reduction of chattering
β	Viscous friction coefficient
σ	Leakage coefficient
η	A positive constant used in sliding mode controller

Note:

\hat{x} signifies the estimation of x and \dot{x} signifies the derivative of the x .

LIST OF FIGURES

Fig. 2.1	Phasor diagram for rotor and stator flux components	15
Fig. 2.2	Induction motor drive system with sensorless speed control scheme	16
Fig. 3.1	The sliding condition	22
Fig. 3.2	Graphical interpretation of equation (3.13) and (3.14)	23
Fig. 3.3	Sliding mode principle with boundary layer	27
Fig. 3.4	Induction motor drive system with sliding mode controller	28
Fig. 4.1	Speed and speed error for Step change in reference speed with P-I controller	31
Fig. 4.2	q- axis stator input voltage and d- and q-axis stator current for Step change in reference speed with P-I controller	32
Fig. 4.3	Stator phase current (I_a) for step change in reference speed with P-I controller	33
Fig. 4.4	Speed response and speed error for Step change in reference speed with Sliding mode controller	34
Fig. 4.5	q- axis stator input voltage and d- and q-axis stator current for Step change in reference speed with Sliding mode controller	35
Fig. 4.6	stator phase current and control input for Step change in reference speed with Sliding mode controller	36
Fig. 4.7	speed response and q- axis stator voltage for trapezoidal speed tracking with P-I controller	37
Fig. 4.8	d- and q-axis stator current and stator phase current for Trapezoidal speed tracking with P-I controller	38
Fig. 4.9	Speed response and speed error for Trapezoidal speed tracking with Sliding mode controller	39
fig. 4.10	q- axis stator voltage and d- and q-axis stator current for trapezoidal speed tracking with Sliding mode controller	40
Fig. 4.11	stator phase current and control input, u for trapezoidal speed tracking with Sliding mode controller	41
Fig.4.12	Performance of the drive system under load torque variation with PI and sliding mode controller	42

Chapter-1

INTRODUCTION

1.1 Introduction

The industrial standard for high performance motion control applications require, four quadrant operation including field weakening, minimum torque ripple, rapid speed recovery under impact load torque and fast dynamic torque and speed responses. DC motors with thyristor converter and simple controller structure have been the traditional choice for most industrial and high performance applications. But they are associated with certain problems related to commutation requirement and maintenance. Low torque to weight ratio and reduced unit capacity add some more negative points to DC machine drives. On the other hand AC motors, especially induction motors are suitable for industrial drives, because of their simple and robust structure, high torque to weight ratio, higher reliability and ability to operate in hazardous environments. However their control is a challenging task because the rotor quantities are not accessible which are responsible for torque production. DC machines are decoupled in terms of flux and torque. Hence control is easy. If it is possible in case of induction motor to control the amplitude and space angle (between rotating stator and rotor fields), in other words to supply power from a controlled source so that the flux producing and torque producing components of stator current can be controlled independently, the motor dynamics can be compared to that of DC motor with fast transient response. Presently introduction of micro-controllers and high switching frequency semiconductor devices, and VLSI technology has led to cost effective sophisticated control strategies.

1.1.1 Scalar control

The name scalar control indicates the magnitude variation of control variables only. The control of an induction motor requires a variable voltage variable frequency power source. With advent of the voltage source inverter (VSI), constant voltage/hertz (V/f) control has become the simplest, cheapest and hence one of the popular methods for speed control of induction motor.

This aims at maintaining the same terminal voltage to frequency ratio so as to give nearly constant flux over wide range of speed variation. Since flux is kept constant the full load torque capability are maintained constant under steady state condition except low speed(when an additional voltage boost is needed to compensate for stator winding voltage drop).In this control scheme, the performance of machine improves in the steady state only, but the transient response is poor. More over Constant voltage/hertz control keeps the stator flux linkage constant in steady state with out maintaining decoupling between the flux and torque. So due to inherent coupling effect the dynamic response of the drive is poor. To avoid open loop speed fluctuation due to variation in load torque and supply voltage, a closed loop V/f speed control scheme with slip regulation is normally used for stable operation of the drive under steady state [1].

Scalar control drives were widely used in industry, because it is simple to implement. But inherently there exists a coupling effect between both flux and torque (both are function of voltage or current and frequency), which gives sluggish response and the system becomes prone to instability. The importance of scalar control drives has diminished now a day because of the superior performance of the vector controlled drives.

1.1.2 Vector control

By splitting the stator current into two orthogonal components, one in the direction of flux linkage, representing magnetizing current or flux component of current, and other perpendicular to the flux linkage, representing the torque component of current, and then by varying both components independently, the induction motor can be treated as a separately excited DC motor. This concept was invented in the beginning of 1970s. The implementation of vector control requires information regarding the magnitude and position of the flux vector. Depending upon the method of acquisition of flux information, the vector control or field oriented control method can be termed as: direct or indirect. In the direct method the position of the flux to which orientation is desired is strictly measured with the help of sensors, or estimated from the machine terminal variables such as speed and stator current/voltage signals. The measured or estimated flux is used in the feedback loop, thus the machine parameters have minimal effect on the overall drive performance. But the measurement of flux using flux sensors necessitates special manufacturing process or modifications in the existing machines. Also direct

field orientation method have its inherent problem at low speed where the voltage drops due to resistances are dominant, and pure integration is difficult to achieve [1].

The indirect vector control was originally proposed in [13], eliminates the direct measurement or computation of rotor flux from the machine terminal variables, but controls its instantaneous flux position by summing the rotor position signal with a commanded slip position signal (also known as slip frequency control or feed forward control scheme). The direction of rotor position need an accurate rotor speed information and the commanded slip position is calculated from the model of the induction motor, that again involves machine parameters which may vary with temperature, frequency and magnetic saturation. To get ideal decoupling, the controller should track the machine parameters and for this various adaptation methods have been proposed [3, 8, 12, 18, 20]. However it has been reported that the controller performance is adequate within normal operating temperatures for most of the high performance applications, and the parameter adaptations methods may be essential only in the case of critical applications. In contrast to direct method the indirect method controls the flux in an open loop manner.

Field orientation scheme can be implemented with reference to any of the three flux vectors: stator flux, air gap flux and rotor flux. It has been shown that out of the three the orientation with respect to rotor flux alone gives a natural decoupling between flux and torque, fast torque response and better stability. Hence in this work orientation along rotor flux is considered.

1.2 Flux Observer and speed Estimation

There are many techniques involved in implementing different types of field oriented control. Most of the methods require precise estimation of either the rotor position or speed. This implies the need for speed sensors such as shaft mounted tacho-generators or digital shaft encoders. The speed sensors increase the cost and size of the drive, lower the system reliability, and also require special attention to measure noise. Some methods (direct field orientation) require the rotor flux, which is measured using Hall effect sensors or search coils. The Hall effect sensors degrade the performance and reliability of the drive system. The estimation of rotor flux by integration of the open loop machine voltages arise difficulties at low speed.

Finally, although the indirect field orientation is simple and preferred, its performance is highly dependent on accurate knowledge of the machine parameters. Research in induction motor control has been focused to remedy the above problems. Much work has been reported in decreasing the sensitivity of the control system to the parameter variation and estimating, rather than measuring the rotor flux and speed from the terminal voltages and currents. This eliminates the flux or speed sensor, thereby achieving sensorless control. Many speed estimation algorithms and speed sensorless control schemes have been developed during the past few years. One of the major problems with the terminal quantities-based flux observers designed in the past is their sensitivity to the machine parameters, specifically, to rotor resistance for the current model observer and to stator resistance in case of the voltage model flux observer. To overcome these problems various control techniques have been tried to improve the rotor flux estimation. Some are discussed below.

The Kalman filter algorithm and its extensions are robust and efficient observers for linear and nonlinear systems respectively. An extended Kalman filter is used in [15] for speed estimation of vector controlled induction motor drive. Unfortunately, this approach contains some inherent disadvantages such as its heavy computational requirements and difficult design and tuning procedure.

A number of Model Reference Adaptive System based speed sensorless schemes have been described in the literature for field oriented induction motor drives [24, 27], where one of the flux estimators acts as a reference model, and the other acts as the adaptive estimator.

Rotor saliency method based on signal injection is one of the techniques to determine rotor position and speed. This has been developed using high frequency measurements based on machine saliencies, rotor slotting and irregularities. High frequency signals are injected into stator terminals. Proper signal processing and filtering of the resulting high frequency stator current are used to detect the induced saliencies present in the stator model of the induction motor. These approaches have been shown to have the potential for wide speed range and parameter insensitive sensorless control, particularly during low speed operation. But the saliency-based technique with fundamental excitation [2, 4] often fails at low and zero speeds. When applied with high frequency signal injection [9, 10], this method may cause torque ripples, vibrations, and audible noise. Also, the saliency-based technique is machine specific.

The direct self control or direct torque control (DTC) [5] is a variation of sensorless field oriented control, where the flux position and the error in flux and torque are directly used to choose the inverter switching state.

Recently, substantial research efforts have also been devoted to intelligent controllers such as artificial neural networks (ANN) and fuzzy logic to deal with the problems of nonlinearity and uncertainty of system parameters. The fundamental characteristics of neural networks are: ability to produce good models of nonlinear systems; highly distributed and paralleled structure, which makes neural-based control schemes faster than traditional ones; simple implementation by software or hardware; and ability to learn and adapt to the behavior of any real process. On the other hand it was shown that fuzzy controllers are capable of improving the tracking performance under external disturbances, or when the IFO drive system experiences imperfect decoupling due to variations in the rotor time constant. Neural network and fuzzy logic are gaining potential as estimators and controllers for many industrial applications, due to the fact that they possess better tracking properties than conventional controllers.

1.3 Necessity of a robust controller

To achieve decoupling is the main aim of vector control. The ideal decoupling will not be obtained, if the rotor parameters used in the decoupling control law can not track their true values. As a result of detuning of rotor parameters, the efficiency of the motor drive is degraded owing to the reduction of torque generating capability and the magnetic saturation caused by over excitation. The dynamic control characteristics are also degraded. On-line adaptation of parameters to achieve decoupling is possible, but very difficult and complex process. To reduce effects of rotor parameter variations, various on-line tuning techniques have been reported [3, 8, 12, 14].

A robust control technique is a good solution for the rotor parameter detuning problem. In addition to the above problem, there are also other problems associated with induction motor drives which necessitate a robust control technique. These are load torque disturbances, approximations in the model used in analysis and design of the controller, and necessity to track complex trajectories, not only step changes. Under these conditions a robust control technique is essential. Sliding Mode is one such control technique.

1.4 Sliding Mode Controller

Sliding mode controller is suitable for a specific class of nonlinear systems. This is applied in the presence of modeling inaccuracies, parameter variation and disturbances, provided that the upper bounds of their absolute values are known. Modeling inaccuracies may come from certain uncertainty about the plant (e.g. unknown plant parameters), or from the choice of a simplified representation of the system dynamic. Sliding mode controller design provides a systematic approach to the problem of maintaining stability and satisfactory performance in presence of modeling imperfections. The sliding mode control is especially appropriate for the tracking control of motors, robot manipulators whose mechanical load change over a wide range. Induction motors are used as actuators which have to follow complex trajectories specified for manipulator movements. Advantages of sliding mode controllers are that it is computationally simple compared adaptive controllers with parameter estimation and also robust to parameter variations. The disadvantage of sliding mode control is sudden and large change of control variables during the process which leads to high stress for the system to be controlled. It also leads to chattering of the system states.

Soto and Yeung [23] and Utkin [25] have applied sliding mode control to induction motor drive. In [7, 25] sliding mode control methods are applied to an indirect vector controlled induction machine for position and speed control. It is also applied in [11] to position control loop of an indirect vector control induction motor drive, without rotor resistance identification scheme. A sliding mode based adaptive input output linearizing control is presented in [21] for induction motor drives. In this case the motor flux amplitude and speed are separately controlled by sliding mode controllers with variable switching gains. A sliding mode controller with rotor flux estimation is presented in [28-29] for induction motor drives. Rotor flux is also estimated using a sliding mode observer.

Although many speed estimation algorithms and sensorless control schemes are developed during the past few years, development of a simple, effective and low sensitivity speed estimation scheme for a low power IM drive is lacking in the literature. Sliding mode controller is a good choice for handling this type of problems.

1.5 Organization of the Thesis

The following presents the outline of the work in details.

Chapter 1 presents a review on the available literature on scalar control and vector control stating their limitations. Various types of observer and speed estimation scheme are also described. The application aspect of sliding mode controller to induction motor drive is also presented. Lastly it sets forth the objectives of the present work and outlines the organization of the thesis.

Modeling of induction motor is discussed in *Chapter 2*. The differential equations of the motor are expressed in synchronously rotating (d- q) reference frame with stator current and rotor flux components as state variables. The developed torque is used as a state variable in place of q- axis stator current. The drive system is transformed to two linear and decoupled subsystems; electrical and mechanical. There are two PI controllers for the mechanical subsystem and one for the electrical.

A reduced order (Gopinath type) rotor flux observer has been designed to estimate rotor flux. This observer estimates both the components of rotor flux in the synchronous reference frame. But the q-axis flux linkage is zero at the steady state and nearly zero during transients. So its computation is not needed and a simpler observer for estimating only the d-axis rotor flux is developed. The computation needed is decreased and thus preferable for real time estimation. A simple, effective and low sensitivity speed estimation technique has been proposed [19] for the drive is described here. The speed is calculated from the estimated stator flux linkage components in the stationary reference frame.

Development of a sliding mode controller for robust control of induction motor drive under model inaccuracy, load disturbances and parameter variations is described in *Chapter 3*. The theory of sliding mode control is briefly reviewed and control law is derived. The controller gain and band width are determined considering various factors, such as rotor resistance variation, model inaccuracy and load disturbances to have an ideal speed tracking. The control law is modified to reduce the chattering of the control input and states. The width of the boundary layer, introduced for this purpose, is determined to reduce chattering as well as to keep the tracking error at its minimum value.

The PI controller and sliding mode controller are simulated for an induction motor drive using Matlab/simulink in *Chapter 4*. The PWM inverter is simulated assuming all the devices to be ideal switches. The results of both the controllers are compared.

Finally in *chapter 5*, some concluding comments summarizing the advantages and limitations of the proposed controller are presented. This also includes few suggestions for future research work.

Chapter- 2

MODELLING OF INDUCTION MOTOR

2.1 Introduction

Although construction of induction motor is simple, its speed control is considered to be far more complex than that of DC motors. The reason is nonlinear and highly interacting multivariable state space model of the motor. The rapid and revolutionary progress in microelectronics and variable frequency static inverters with application of modern control theory has made it possible to build sophisticated controllers for AC motor drives. The design and development of such drive system require proper mathematical modeling of the motor to optimize the controller structure, the inputs needed and the gain parameters. In this chapter the modeling of induction motor is presented.

2.2 Induction Motor Modeling

A proper model for the three phase induction motor is essential to simulate and study the complete drive system. The model of induction motor in arbitrary reference frame is derived in [16-17].

Following are the assumptions made for the model:

1. Each stator winding is distributed so as to produce a sinusoidal mmf along the airgap, i.e. space harmonics are negligible.
2. The slotting in stator and rotor produces negligible variation in respective inductances.
3. Mutual inductances are equal.
4. The harmonics in voltages and currents are neglected.
5. Saturation of the magnetic circuit is neglected.
6. Hysteresis and eddy current losses and skin effects are neglected.

The voltage equations of the three phase induction motor in synchronous reference frame are:

$$v_{ds} = R_s i_{ds} + \frac{d\psi_{ds}}{dt} - \omega_e \psi_{qs} \quad (2.1)$$

$$v_{qs} = R_s i_{qs} + \frac{d\psi_{qs}}{dt} + \omega_e \psi_{ds} \quad (2.2)$$

$$v_{dr} = R_r i_{dr} + \frac{d\psi_{dr}}{dt} - (\omega_e - P\omega_r)\psi_{qr} \quad (2.3)$$

$$v_{qr} = R_r i_{qr} + \frac{d\psi_{qr}}{dt} + (\omega_e - P\omega_r)\psi_{dr} \quad (2.4)$$

The developed torque T_e is:

$$T_e = \frac{3}{2}P(\psi_{ds}i_{qs} - \psi_{qs}i_{ds}) \quad (2.5)$$

The torque balance equation is:

$$J \frac{d\omega_r}{dt} = T_e - T_l - \beta\omega_r \quad (2.6)$$

Where, in the above equations, all voltages (v) and currents (i) refer to the arbitrary reference frame. The subscripts ds, qs, dr and qr corresponds to d and q-axis quantities for the stator and rotor respectively. Ψ denotes flux linkage. ω_e and ω_r are the speed of the reference frame and the mechanical speed of the rotor in rad/sec. R_s and R_r are the stator and rotor resistances per phase of the motor respectively. P is the number of pole pairs. J is the moment of inertia and β is the coefficient of viscous friction. T_e is the developed torque and T_l is the load torque.

The above equations can be written in matrix form as follows:

$$\begin{bmatrix} v_{ds} \\ v_{qs} \end{bmatrix} = \begin{bmatrix} R_s & 0 \\ 0 & R_s \end{bmatrix} \begin{bmatrix} i_{ds} \\ i_{qs} \end{bmatrix} + \frac{d}{dt} \begin{bmatrix} \psi_{ds} \\ \psi_{qs} \end{bmatrix} + \begin{bmatrix} 0 & -\omega_e \\ \omega_e & 0 \end{bmatrix} \begin{bmatrix} \psi_{ds} \\ \psi_{qs} \end{bmatrix} \quad (2.7)$$

$$\begin{bmatrix} v_{dr} \\ v_{qr} \end{bmatrix} = \begin{bmatrix} R_r & 0 \\ 0 & R_r \end{bmatrix} \begin{bmatrix} i_{dr} \\ i_{qr} \end{bmatrix} + \frac{d}{dt} \begin{bmatrix} \psi_{dr} \\ \psi_{qr} \end{bmatrix} + \begin{bmatrix} 0 & -(\omega_e - P\omega_r) \\ (\omega_e - P\omega_r) & 0 \end{bmatrix} \begin{bmatrix} \psi_{dr} \\ \psi_{qr} \end{bmatrix} \quad (2.8)$$

$$T_e = \frac{3}{2}P[\psi_{ds} \quad \psi_{qs}] \begin{bmatrix} i_{qs} \\ -i_{ds} \end{bmatrix} \quad (2.9)$$

Squirrel cage induction motor is mostly used and its rotor windings are short circuited,

$$\begin{bmatrix} v_{dr} \\ v_{qr} \end{bmatrix} = \begin{bmatrix} 0 \\ 0 \end{bmatrix} \quad (2.10)$$

neglecting iron losses, the flux linkage equations in matrix form are

$$\begin{bmatrix} \psi_{ds} \\ \psi_{qs} \end{bmatrix} = \begin{bmatrix} L_s & 0 \\ 0 & L_s \end{bmatrix} \begin{bmatrix} i_{ds} \\ i_{qs} \end{bmatrix} + \begin{bmatrix} L_m & 0 \\ 0 & L_m \end{bmatrix} \begin{bmatrix} i_{dr} \\ i_{qr} \end{bmatrix} \quad (2.11)$$

$$\begin{bmatrix} \psi_{dr} \\ \psi_{qr} \end{bmatrix} = \begin{bmatrix} L_m & 0 \\ 0 & L_m \end{bmatrix} \begin{bmatrix} i_{ds} \\ i_{qs} \end{bmatrix} + \begin{bmatrix} L_r & 0 \\ 0 & L_r \end{bmatrix} \begin{bmatrix} i_{dr} \\ i_{qr} \end{bmatrix} \quad (2.12)$$

Where L_s and L_r self inductances of stator and rotor respectively and L_m is the mutual inductance between stator and rotor.

From equation (2.12)

$$\begin{bmatrix} i_{dr} \\ i_{qr} \end{bmatrix} = \begin{bmatrix} \frac{1}{L_r} & 0 \\ 0 & \frac{1}{L_r} \end{bmatrix} \begin{bmatrix} \psi_{dr} \\ \psi_{qr} \end{bmatrix} - \begin{bmatrix} \frac{L_m}{L_r} & 0 \\ 0 & \frac{L_m}{L_r} \end{bmatrix} \begin{bmatrix} i_{ds} \\ i_{qs} \end{bmatrix} \quad (2.13)$$

Substituting (2.13) in (2.11),

$$\begin{aligned} \begin{bmatrix} \psi_{ds} \\ \psi_{qs} \end{bmatrix} &= \begin{bmatrix} \left(L_s - \frac{L_m^2}{L_r} \right) & 0 \\ 0 & \left(L_s - \frac{L_m^2}{L_r} \right) \end{bmatrix} \begin{bmatrix} i_{ds} \\ i_{qs} \end{bmatrix} + \begin{bmatrix} \frac{L_m}{L_r} & 0 \\ 0 & \frac{L_m}{L_r} \end{bmatrix} \begin{bmatrix} \psi_{dr} \\ \psi_{qr} \end{bmatrix} \\ &= \begin{bmatrix} \sigma L_s & 0 \\ 0 & \sigma L_s \end{bmatrix} \begin{bmatrix} i_{ds} \\ i_{qs} \end{bmatrix} + \begin{bmatrix} \frac{L_m}{L_r} & 0 \\ 0 & \frac{L_m}{L_r} \end{bmatrix} \begin{bmatrix} \psi_{dr} \\ \psi_{qr} \end{bmatrix} \end{aligned} \quad (2.14)$$

Where $\sigma = 1 - \frac{L_m^2}{L_s L_r} =$ Leakage coefficient.

Using (2.10) and substituting (2.13) in (2.8) and then re arranging, we get

$$\frac{d}{dt} \begin{bmatrix} \psi_{dr} \\ \psi_{qr} \end{bmatrix} = \begin{bmatrix} \frac{R_r L_m}{L_r} & 0 \\ 0 & \frac{R_r L_m}{L_r} \end{bmatrix} \begin{bmatrix} i_{ds} \\ i_{qs} \end{bmatrix} + \begin{bmatrix} -\frac{R_r}{L_r} & 0 \\ 0 & -\frac{R_r}{L_r} \end{bmatrix} \begin{bmatrix} \psi_{dr} \\ \psi_{qr} \end{bmatrix} + \begin{bmatrix} 0 & -(\omega_e - P\omega_r) \\ (\omega_e - P\omega_r) & 0 \end{bmatrix} \begin{bmatrix} \psi_{dr} \\ \psi_{qr} \end{bmatrix}$$

or

$$\frac{d}{dt} \begin{bmatrix} \psi_{dr} \\ \psi_{qr} \end{bmatrix} = \begin{bmatrix} a_5 & 0 \\ 0 & a_5 \end{bmatrix} \begin{bmatrix} i_{ds} \\ i_{qs} \end{bmatrix} + \begin{bmatrix} -a_4 & \omega_{sl} \\ \omega_{sl} & -a_4 \end{bmatrix} \begin{bmatrix} \psi_{dr} \\ \psi_{qr} \end{bmatrix} \quad (2.15)$$

Where $a_5 = \frac{R_r L_m}{L_r}$, $a_4 = \frac{R_r}{L_r}$ and $\omega_{sl} = \omega_e - P\omega_r$ (2.15a)

Substituting (2.14) in (2.7) and again substituting (2.15) and then simplifying and rearranging, we get

$$\frac{d}{dt} \begin{bmatrix} i_{ds} \\ i_{qs} \end{bmatrix} = \begin{bmatrix} -a_1 & \omega_e \\ -\omega_e & -a_1 \end{bmatrix} \begin{bmatrix} i_{ds} \\ i_{qs} \end{bmatrix} + \begin{bmatrix} a_2 & Pa_3\omega_r \\ -Pa_3\omega_r & a_2 \end{bmatrix} \begin{bmatrix} \psi_{dr} \\ \psi_{qr} \end{bmatrix} + \begin{bmatrix} c & 0 \\ 0 & c \end{bmatrix} \begin{bmatrix} v_{ds} \\ v_{qs} \end{bmatrix} \quad (2.16)$$

Where

$$\begin{aligned} a_1 &= \frac{1}{\sigma L_s} (R_s + R_r \frac{L_m^2}{L_r^2}) , \\ a_2 &= \frac{1}{\sigma L_s} R_r \frac{L_m^2}{L_r^2} , \\ a_3 &= \frac{1}{\sigma L_s} \frac{L_m}{L_r} \\ c &= \frac{1}{\sigma L_s} \end{aligned} \quad (2.16a)$$

Combining (2.15) and (2.16), the state space model of the induction motor in terms of stator current and rotor flux linkages is given as follows:

$$\frac{d}{dt} \begin{bmatrix} i_{ds} \\ i_{qs} \\ \psi_{dr} \\ \psi_{qr} \end{bmatrix} = \begin{bmatrix} -a_1 & \omega_e & a_2 & Pa_3\omega_r \\ -\omega_e & -a_1 & -Pa_3\omega_r & a_2 \\ a_5 & 0 & -a_4 & \omega_{sl} \\ 0 & a_5 & -\omega_{sl} & -a_4 \end{bmatrix} \begin{bmatrix} i_{ds} \\ i_{qs} \\ \psi_{dr} \\ \psi_{qr} \end{bmatrix} + \begin{bmatrix} c & 0 \\ 0 & c \\ 0 & 0 \\ 0 & 0 \end{bmatrix} \begin{bmatrix} v_{ds} \\ v_{qs} \end{bmatrix} \quad (2.17)$$

Using (2.14) and (2.9) and simplifying, we get

$$T_e = \frac{3}{2} P \frac{L_m}{L_r} [\psi_{dr} \quad \psi_{qr}] \begin{bmatrix} i_{qs} \\ -i_{ds} \end{bmatrix}$$

or $T_e = \frac{3}{2} P \frac{L_m}{L_r} [\psi_{dr} i_{qs} - \psi_{qr} i_{ds}]$ (2.18)

2.3 The Field Oriented control

To achieve field orientation along the rotor flux, the flux component (d-axis component) of stator current, i_{ds} is aligned in the direction of rotor flux, ψ_r , and the torque component of stator current, i_{qs} is aligned in direction perpendicular to it. At this condition:

$$\psi_{qr} = 0 \text{ and } \frac{d\psi_{qr}}{dt} = 0 \quad (2.19)$$

$$\Psi_{dr} = \Psi_r = \text{rotor flux.}$$

Hence the developed electromagnetic torque is given by:

$$T_e = \frac{3P}{2} \frac{L_m}{L_r} \psi_{dr} i_{qs} = K_t \psi_{dr} i_{qs} \quad (2.20)$$

With field orientation, the dynamic behavior of the induction machine is given by:

$$\frac{di_{ds}}{dt} = -a_1 i_{ds} + a_2 \psi_{dr} + \omega_e i_{qs} + c v_{ds} \quad (2.21)$$

$$\frac{di_{qs}}{dt} = -\omega_e i_{ds} - a_1 i_{qs} - P a_3 \omega_r \psi_{dr} + c v_{qs} \quad (2.22)$$

$$\frac{d\psi_{dr}}{dt} = -a_4 \psi_{dr} + a_5 i_{ds} \quad (2.23)$$

Slip frequency for obtaining indirect field orientation is given by :

$$\omega_{sl} = \omega_e - P\omega_r = a_5 \cdot \frac{i_{qs}}{\psi_{dr}} \quad (2.24)$$

Where $a_5 = \frac{R_r L_m}{L_r}$

With these conditions the decoupling of torque and flux is guaranteed in field oriented control and it can be controlled linearly as a separately excited DC motor. However due to the presence of rotor time constant (R_r/L_r) in equation (2.24), the indirect field orientation control is highly parameter sensitive. Along with this, unpredictable parameter variations, external load disturbances, unmodelled and nonlinear dynamics adversely affect the control performance of the drive system.

2.4 Estimation of Speed

It is desirable to avoid the use of speed sensors from the standpoints of cost, size of the drive, noise immunity and reliability. So the development of shaft sensorless adjustable speed drive has become an important research topic. Many speed estimation algorithms and sensorless control schemes [22] have been developed during the past few years. The speed information required in the proposed control technique is estimated by the algorithm described in this section. The speed of the motor is estimated by estimating the synchronous speed and subtracting the command slip speed. The synchronous speed is estimated using the stator flux components, because of its higher accuracy compared to estimation based on rotor flux components.

The rotor speed of an induction motor is expressed in terms of synchronous and slip (angular) frequencies is as follows:

$$\omega_r = \frac{\omega_e - \omega_{sl}}{P}$$

The estimation of rotor speed is accomplished by an estimation of either synchronous, or slip frequency, with the other being known. In the proposed speed estimation scheme, the synchronous frequency is estimated and slip frequency is assumed as command. So the estimated rotor speed of the sensorless drive is obtained from the above equation as:

$$\hat{\omega}_r = \frac{\hat{\omega}_e - \omega_{sl}^*}{P}$$

Where,

$\hat{\omega}_r$ = estimated rotor frequency in rad/sec.

$\hat{\omega}_e$ = estimated synchronous frequency in rad/sec.

ω_{sl}^* = command value of slip frequency in rad/sec.

The estimated synchronous frequency is derived based on the rotor flux model, or the stator flux model. The principles of both the methods are briefly explained bellow.

If $\psi_{\beta r}$ and $\psi_{\alpha r}$ are the two components of the rotor flux vector in the stationary (α - β) reference frame as shown in Fig. 2.1 (a), the electrical angle of the rotor flux vector is defined as:

$$\theta_{\psi_r} = \tan^{-1} \left(\frac{\psi_{\beta r}}{\psi_{\alpha r}} \right)$$

The derivative of this rotor flux angle (with respect to time) gives the instantaneous angular frequency.

$$\omega_e = \dot{\theta}_{\psi_r} = \frac{\psi_{\alpha r} \dot{\psi}_{\beta r} - \psi_{\beta r} \dot{\psi}_{\alpha r}}{\psi_{\alpha r}^2 + \psi_{\beta r}^2}$$

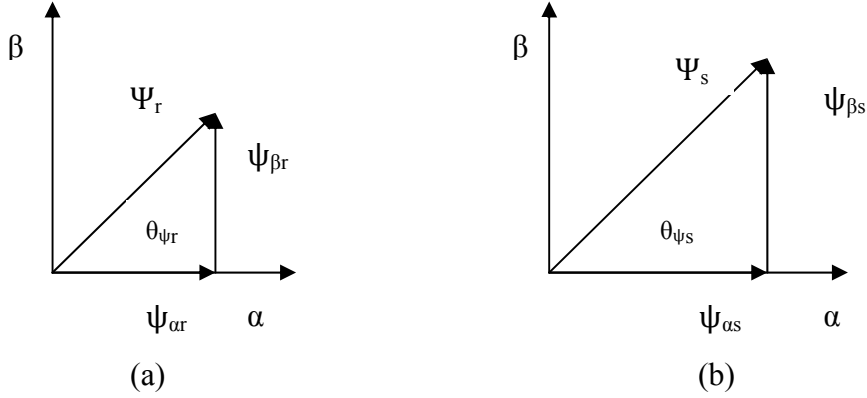


Fig. 2.1 Phasor diagram for rotor and stator flux components

If $\psi_{\beta s}$ and $\psi_{\alpha s}$ are the two components of the stator flux vector in the stationary (α - β) reference frame as shown in Fig. 2.1(b) the electrical angle of the stator flux vector is defined as:

$$\theta_{\psi_s} = \tan^{-1} \left(\frac{\psi_{\beta s}}{\psi_{\alpha s}} \right)$$

The derivative of this rotor flux angle (with respect to time) gives the instantaneous angular frequency.

$$\omega_e = \dot{\theta}_{\psi_s} = \frac{\psi_{\alpha s} \dot{\psi}_{\beta s} - \psi_{\beta s} \dot{\psi}_{\alpha s}}{\psi_{\alpha s}^2 + \psi_{\beta s}^2}$$

From the basic equation of induction motor in stationary (α - β) reference frame, the stator and rotor flux linkages are given by

$$\begin{aligned} \psi_{\alpha s} &= \int_0^t (v_{\alpha s} - R_s i_{\alpha s}) dt \\ \psi_{\beta s} &= \int_0^t (v_{\beta s} - R_s i_{\beta s}) dt \end{aligned} \quad (2.25)$$

$$\begin{aligned} \psi_{\alpha r} &= \frac{L_r}{L_m} (\psi_{\alpha s} - \sigma L_s i_{\alpha s}) \\ \psi_{\beta r} &= \frac{L_r}{L_m} (\psi_{\beta s} - \sigma L_s i_{\beta s}) \end{aligned} \quad (2.26)$$

Equation (2.25) shows that the stator flux depends on the stator resistance and measured stator voltages and currents. Equation (2.26) shows that the rotor flux depends on the estimated stator flux and requires the knowledge of the inductances of the machine, especially the stator leakage inductance (σL_s). Usually the stator resistance can be measured fairly accurately. Hence stator flux can be estimated more accurately compared to the rotor flux. Therefore the estimated stator flux can be used to derive the synchronous frequency.

The block diagram of the described speed estimation algorithm with the sensorless speed control scheme is shown in fig 2.2

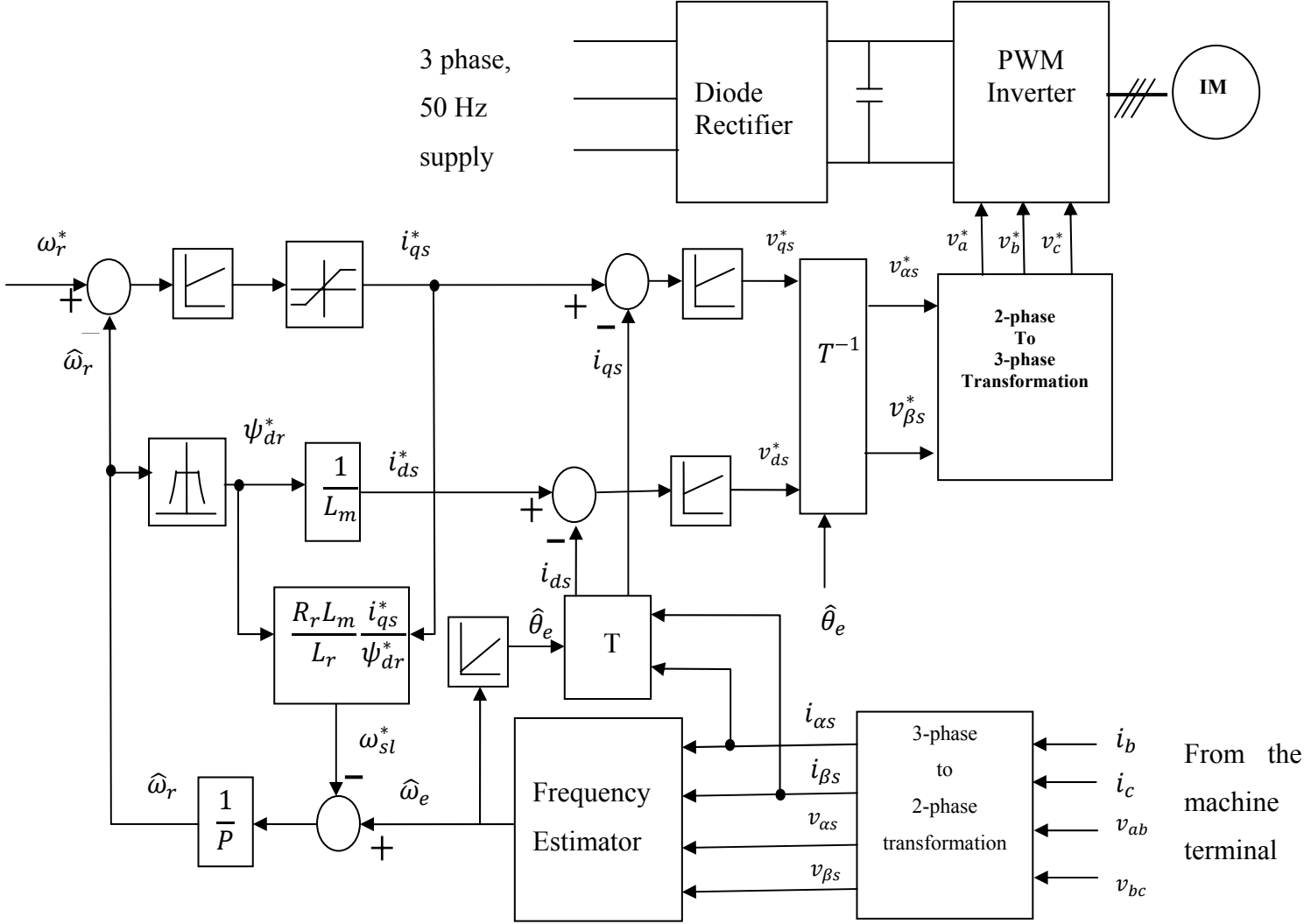


Fig 2.2 Induction motor drive system with sensorless speed control scheme

2.5 Chapter Conclusion

In this chapter the induction motor model in arbitrary reference frame is discussed in detail. Because a dynamic model of the machine subjected to control must be known in order to understand and design vector controlled drives. Condition to achieve indirect vector control is derived. The speed estimation algorithm is studied in detail in order to apply the sensorless technique in the present drive system.

Chapter – 3

DESIGN OF A SLIDING MODE CONTROLLER

3.1 Introduction

In control theory sliding mode control, is a form of variable structure control (VSC). It is a nonlinear control method that alters the dynamics of a nonlinear system by application of a high-frequency switching control. The multiple control structures are designed so that trajectories always move toward a switching condition, and hence the ultimate trajectory will not exist entirely within one control structure. Instead, the ultimate trajectory will slide along the boundaries of the control structures. The motion of the system as it slides along these boundaries is called a sliding mode.

Intuitively, for a dynamic system sliding mode control uses practically infinite gain to force the trajectories to slide along the restricted sliding mode subspace. The main strength of sliding mode control is its robustness. Because the control can be as simple as a switching between two states (e.g., "on"/"off" or "forward"/"reverse"), it need not be precise and will not be sensitive to parameter variations that enter into the control channel. Additionally, because the control law is not a continuous function, the sliding mode can be reached in finite time (i.e., better than asymptotic behavior). Sliding mode control is an appropriate robust control method for the systems, where modeling inaccuracies, parameter variations and disturbances are present. It is computationally simple compared to adaptive controllers with parameter estimation. Induction motor with sliding mode control performs well in the servo applications, where the actuator has to follow complex trajectories. Sometimes sliding mode control has a demerit of chattering of the control variable and some of the system states.

The strengths of SMC include:

- Low sensitivity to plant parameter uncertainty
- Greatly reduced-order modeling of plant dynamics
- Finite-time convergence (due to discontinuous control law)

The weaknesses of SMC include:

- Chattering due to implementation imperfections

3.2 sliding Mode Controller

With sliding mode controller, the system is controlled in such a way that the error in the system states always moves towards a sliding surface. The sliding surface is defined with the tracking error (e) of the state and its rate of change (e') as variables. The distance of the error trajectory from the sliding surface and its rate of convergence are used to decide the control input (u) to the system. The sign of the control input must change at the intersection of the tracking error trajectory with the sliding surface. In this way the error trajectory is always forced to move towards the sliding surface.

The basic equations (2.20 – 2.24) of vector controlled induction motor are simplified by assuming, the rotor flux ψ_{dr} to be constant. From (2.23) the steady state value of the rotor flux can be obtained as

$$\psi_{dr}^* = \frac{a_5}{a_4} i_{ds}^* \quad (3.1)$$

From (2.15a), we get

$$\frac{a_5}{a_4} = L_m \quad (3.1a)$$

Using (3.1a) in (3.1), steady state value of rotor flux is obtained as

$$\psi_{dr}^* = L_m i_{ds}^* \quad (3.1b)$$

The speed dynamic equation is given by

$$\frac{d\omega_r}{dt} = \frac{1}{J} (T_e - T_l - \beta\omega_r) \quad (3.2)$$

Using (2.20) in (3.2) we get,

$$\dot{\omega}_r = \frac{1}{J} (K_T \psi_{dr}^* i_{qs} - \beta\omega_r - T_l)$$

Assuming the load torque, T_l to be a disturbance to a system, the speed dynamic equation is simplified as:

$$\dot{\omega}_r = -\frac{\beta}{J}\omega_r + b i_{qs} + noise \quad (3.3)$$

or

$$\dot{\omega}_r = f_1 + noise \quad (3.3a)$$

Where,

$$f_1 = -\frac{\beta}{J}\omega_r + b i_{qs} \quad (3.4)$$

and

$$b = \frac{K_T}{J} \psi_{dr}^* \quad (3.4a)$$

In this vector controlled induction motor drive, speed is taken as the output variable. To track the speed accurately in the second order speed control system, the conditions to be satisfied are:

$$\dot{\omega}_r |_{\omega_r = \omega_r^*} = 0 \quad \text{and} \quad \ddot{\omega}_r |_{\omega_r = \omega_r^*} = 0 \quad (3.5)$$

From equation (4.2)

$$\ddot{\omega}_r = -\frac{\beta}{J}\dot{\omega}_r + b \dot{i}_{qs} + noise \quad (3.5a)$$

Substituting $\omega_e = P\omega_r + a_5 \cdot \frac{i_{qs}}{\psi_{dr}}$ in (2.22), the following equation is obtained.

$$\dot{i}_{qs} = -\left(P\omega_r + a_4 \frac{i_{qs}}{i_{ds}}\right) i_{ds} - a_1 i_{qs} - P a_3 \omega_r L_m i_{ds} + c v_{qs} \quad (3.6)$$

It can be shown using (2.24) and (3.1), that

$$\omega_{sl} = a_5 \frac{i_{qs}}{\psi_{dr}^*} = \frac{R_r L_m}{L_r} \frac{i_{qs}}{L_m i_{ds}^*} \approx a_4 \frac{i_{qs}}{i_{ds}}$$

Simplifying (3.6), we get

$$\dot{i}_{qs} = -(a_1 + a_4) i_{qs} - P\omega_r(1 + a_3 L_m) i_{ds} + c v_{qs}$$

or

$$\dot{i}_{qs} = f_2 + c v_{qs} \quad (3.6a)$$

Where

$$f_2 = -(a_1 + a_4) i_{qs} - P\omega_r(1 + a_3 L_m) i_{ds} \quad (3.7)$$

Substituting (3.2) and (3.6a) in (3.5a), we get

$$\ddot{\omega}_r = -\frac{\beta}{J}f_1 + bf_2 + bc v_{qs} + d$$

or

$$\ddot{\omega}_r = G + u + d \quad (3.8)$$

Where

d = total disturbance

$$\text{and } u = b c v_{qs} = \text{control input.} \quad (3.8a)$$

$$\text{and } G = -\frac{\beta}{J}f_1 + bf_2 \quad (3.9)$$

G is a function, which can be estimated from measured values of current and speed.

u is directly proportional to v_{qs} and decides the modulating signal and hence output voltage of the PWM voltage source inverter.

Let

$$G = \hat{G} + \Delta G \quad (3.10)$$

Where \hat{G} is an approximate estimate of G , and ΔG is the estimation error due to modeling imperfection.

The control problem is to obtain the system states,

$$X = [\omega_r \quad \dot{\omega}_r]^T$$

to track a specific time varying state,

$$X^* = [\omega_r^* \quad \dot{\omega}_r^*]^T$$

in the presence of modeling imperfection and disturbances.

$$\text{Let } e = \omega_r - \omega_r^* \quad (3.11)$$

$$\text{and } \dot{e} = \dot{\omega}_r - \dot{\omega}_r^* \quad (3.12)$$

be the tracking error in the speed and its rate of change respectively.

Let $E = [e \quad \dot{e}]^T$ be the tracking error vector.

A time varying surface, $s(t)$ is defined in the state space by the scalar equation ,

$$s(x, t) = 0$$

$$\text{Where } s(x, t) = \left(\frac{d}{dt} + \lambda\right)e = \dot{e} + \lambda e \quad (3.13)$$

Where λ is a positive constant, which determines the band width of the system.

Starting from the initial condition, $E(0) = 0$, the tracking task, $X \rightarrow X^*$, which means x has to follow X^* with a predefined precision, is considered as solved, if the state vector, E remains in the sliding surface, $S(t)$ for all $t \geq 0$ and also implies that scalar quantity s is kept at zero. A sufficient condition for this behavior is to choose the control law, u of (3.8) and (3.8a) so that

$$\frac{1}{2} \frac{d}{dt}(s^2) \leq -\eta|s| \quad (3.14)$$

Where η is a positive constant. The value of η determines the degree to which the system state is attracted to the switching line. Essentially, equation (3.14) states that the squared distance to the sliding surface, as measured by s^2 decreases along all system trajectories. Thus it constrains the trajectories to point towards the surface $S(t)$, as shown in the figure below [11].

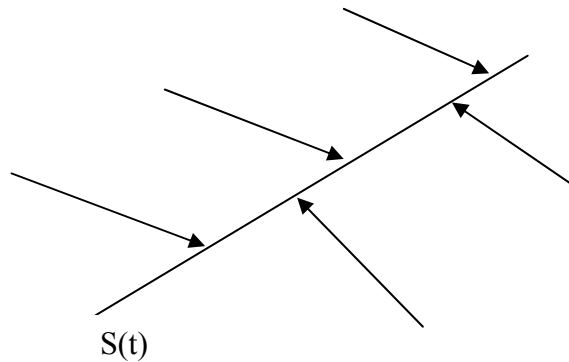


Fig.3.1 The sliding condition

For a second order system, the switching surface is a line and different control structures are applied according to the position of the tracking error vector with respect to the line. The control is designed to drive the state in to the switching line, and once in the line the system state is considered to remain on the line. The state trajectory is defined by the algebraic equation of the line.

Equation (3.14) is the ‘sliding condition’. $S(t)$ satisfying (3.14) is referred to as a sliding surface. And the behavior of the system, once on the surface is called ‘sliding mode’.

Graphical interpretation of equations (3.13) and (3.14) is shown in Fig. 3.2

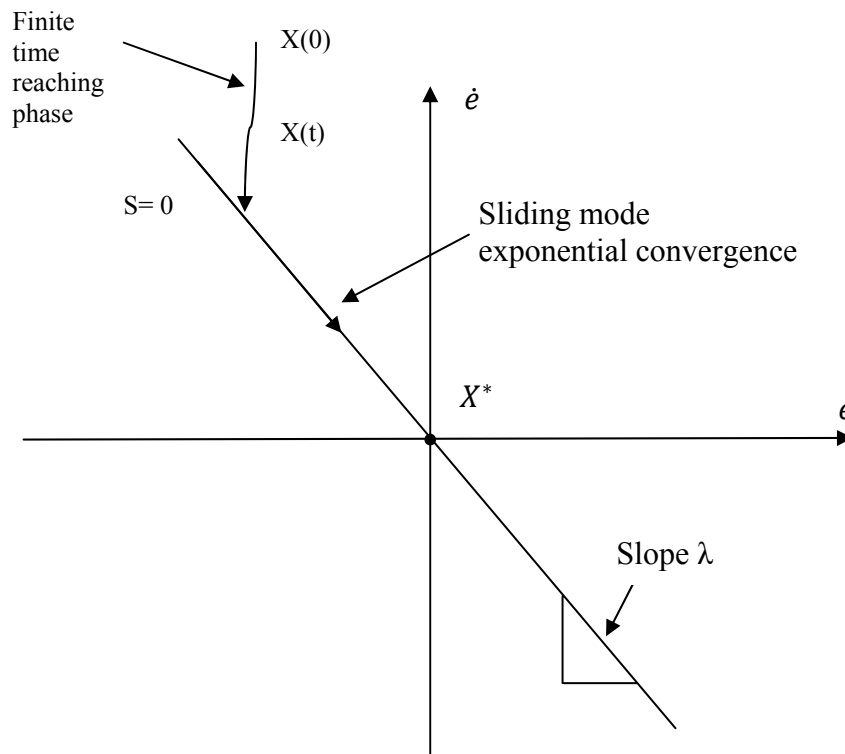


Fig. 3.2 Graphical interpretation of equation (3.13) and (3.14)

Starting from any initial condition, the state trajectory reaches the sliding surface in a finite time smaller than $\frac{|s(t=0)|}{\eta}$, and then slides along the surface towards X^* exponentially with a time constant equal to $1/\lambda$. In the sliding mode, behavior of the system is invariant despite modeling imperfections, parameter variation and disturbances. However the sliding mode causes drastic changes of the control variable, which is a major drawback for the system.

3.2.1 Derivation of Control Law

Referring to equation (4.13), the condition for sliding mode is

$$s \cdot \dot{s} \leq -\eta |s|$$

or alternatively, $\dot{s} \cdot \text{sgn}(s) \leq -\eta$ (3.15)

where

$$\text{sgn}(s) = \begin{cases} 1 & \text{if } s > 0 \\ -1 & \text{if } s \leq 0 \end{cases}$$

From equation (4.12) and (4.11)

$$\dot{s} = \lambda \dot{e} + \ddot{e} = \lambda \dot{e} + \ddot{\omega}_r - \ddot{\omega}_r^* \quad (3.16)$$

Substituting (3.8) in (3.16),

$$\dot{s} = \lambda \dot{e} + G + u + d - \ddot{\omega}_r^* \quad (3.17)$$

Substituting (4.16) in (4.14) and simplifying,

$$(G + d + \lambda \dot{e} - \ddot{\omega}_r^*) \text{sgn}(s) + u \cdot \text{sgn}(s) \leq -\eta \quad (3.18)$$

To achieve the sliding mode of (4.14), u is chosen, so that

$$u = (-\hat{G} - \lambda \dot{e}) - K \cdot \text{sgn}(s) \quad (3.19)$$

Where the gain, K is a positive constant. The first term in (3.19), $(-\hat{G} - \lambda \dot{e})$ is a compensation term and second term is the controller. The compensation term is continuous and reflects the knowledge of system dynamics. The controller term is discontinuous and ensures the sliding to occur.

3.2.2 Design of Controller Gain

Substituting (4.18) in (4.17), we have

$$(G - \hat{G} + d - \ddot{\omega}_r^*) \text{sgn}(s) - K \leq -\eta \quad (3.20)$$

or

$$K \geq (|\Delta G_{max}| + |d_{max}| + \eta + v) \quad (3.21)$$

Where,

$|\Delta G_{max}|$ = upper bound of the estimation error, $(G - \hat{G})$

$|d_{max}|$ = upper bound of the noise, d, and

v = upper bound of command acceleration, $\ddot{\omega}_r^*$

The controller gain K is determined from the maximum amount of imperfection in the estimation process and maximum noise due to parameter variations and disturbance (load torque). If modeling imperfection and parameter variation is large, the value of K should be large. Then discontinuous or switched component ($K \cdot \text{sgn}(s)$) has a more dominant role than the continuous or compensation component, $(-\hat{G} - \lambda \dot{e})$ and lead to chattering. Conversely, better knowledge of the system model and parameter values reduces gain, K and results smooth control response. If large control bandwidth is available, poor knowledge of dynamic model may lead to respectable tracking performance, and hence large modeling efforts may produce only minor improvement in tracking accuracy.

3.2.3 Reduction of Chattering

In a system, where modeling imperfection, parameter variations and amount of noise are more, the value of K must be large to obtain a satisfactory tracking performance with sliding mode controller. But larger value of K leads to more chattering of the control variable and system states. A boundary layer of definite width on both sides of switching line is introduced to reduce chattering. If ϕ is the width of the boundary layer on either side of the switching line, as shown in fig. 3.3, the control law of (3.19) is modified as:

$$u = -\hat{G} - \lambda \dot{e} - K \cdot \text{sat}\left(\frac{s}{\phi}\right) \quad (3.22)$$

Where

$$\text{sat}\left(\frac{s}{\phi}\right) = \begin{cases} \frac{s}{\phi} & \text{if } |s| \leq \phi \\ \text{sgn}(s) & \text{if } |s| > \phi \end{cases}$$

This accounts to a reduction of the control gain inside the boundary layer and results in a smooth control signal.

3.2.4 Design of Bandwidth, λ

From equation (4.21), for $|s| \leq \phi$, ($-\phi \leq s \leq \phi$)

$$u + \lambda \dot{e} + G = \Delta G - K \frac{s}{\phi} \quad (3.23)$$

Substituting equation (3.23) in (3.17), the filter function is obtained as

$$\dot{s} + K \frac{s}{\phi} = \Delta G + d - \ddot{w}_r^* \quad (3.24)$$

Where d is the disturbance and ΔG is the model imperfection.

Suppose the solution of the filter equation (3.24) is s_0 . Then the distance from the state vector, E to the switching line, $s=0$ is:

$$d_1 = |s_0| \frac{1}{\sqrt{1 + \lambda^2}} \quad (3.25)$$

Since slope of the switching line, $s=0$ is λ , the guaranteed tracking precision is:

$$\theta = \frac{\phi}{\lambda} \quad (3.26)$$

The break frequency, v of filter (3.24) is:

$$v = \frac{K_{max}}{\phi} \quad (3.27)$$

The design rule for bandwidth, λ is that the largest acceptable value of λ should be more than or equal to the break frequency, v of filter (3.24). From (3.27) the balance condition is obtained as:

$$v = \frac{K_{max}}{\phi} = \lambda \quad (3.28)$$

This case corresponds to critical damping. Further more the design rule for λ with regard to sample rate, f_{sample} and time constant, τ_{plant} of the plant is denoted as

$$\lambda < \frac{f_{sample}}{2(1 + \tau_{plant} \cdot f_{sample})} \quad (3.29)$$

λ is selected keeping equations (3.26), (3.28) and (3.29) in view. The ratio of boundary layer (ϕ) to bandwidth (λ) should be as small as possible, the ratio being equal to specified tracking precision. Their product should be equal to the maximum value of controller gain, K_{max} . If time constant of the system is known, λ should satisfy (3.29).

To have a tracking precision, $\theta = 1$ rad/sec, from (3.26)

$$\phi = \theta \lambda = \lambda \quad (3.30)$$

From (3.28) $K_{max} = \phi\lambda = \lambda^2$

Hence $\lambda = \sqrt{K_{max}}$

From equation (3.8a)

$$v_{qs}^* = \{(-\hat{G} - \lambda\dot{e} - \ddot{\omega}_r^*)/\hat{b}\} - K \operatorname{sgn}(s) \quad (3.31)$$

without boundary layer.

And with boundary layer it is given by,

$$v_{qs}^* = \{(-\hat{G} - \lambda\dot{e} - \ddot{\omega}_r^*)/\hat{b}\} - K \operatorname{sgn}\left(\frac{s}{\phi}\right) \quad (3.32)$$

Where \hat{b} is the estimate of voltage gain parameter b , which is unknown but has known bounds.

$$0 < b_{min} \leq b \leq b_{max}$$

Here \hat{b} is the geometric mean of the above bounds.

$$\hat{b} = \sqrt{b_{min} b_{max}}$$

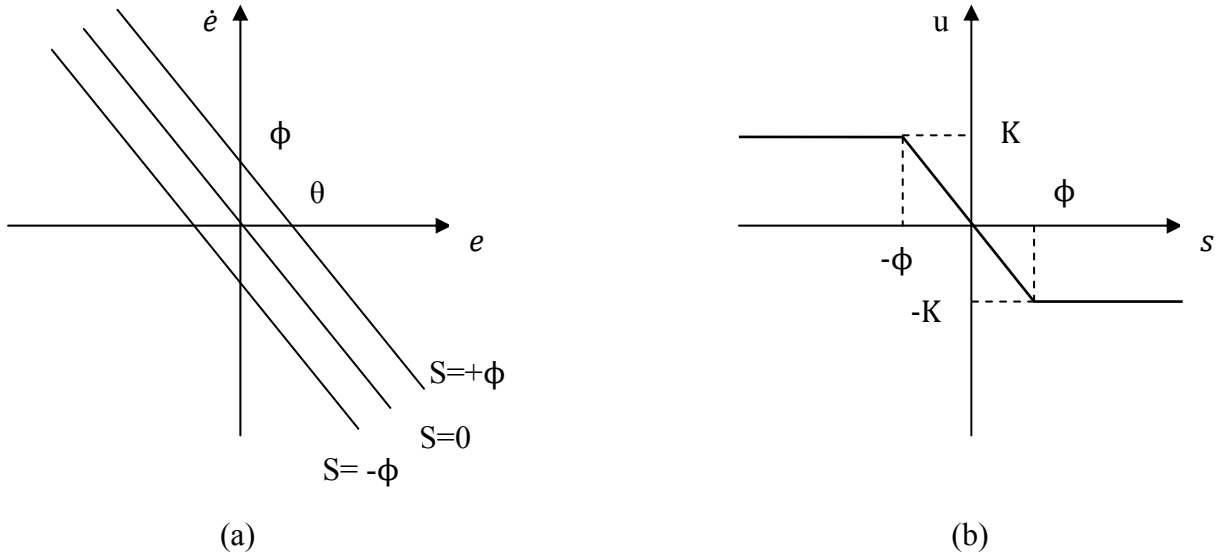


Fig. 3.3 sliding mode principle with boundary layer

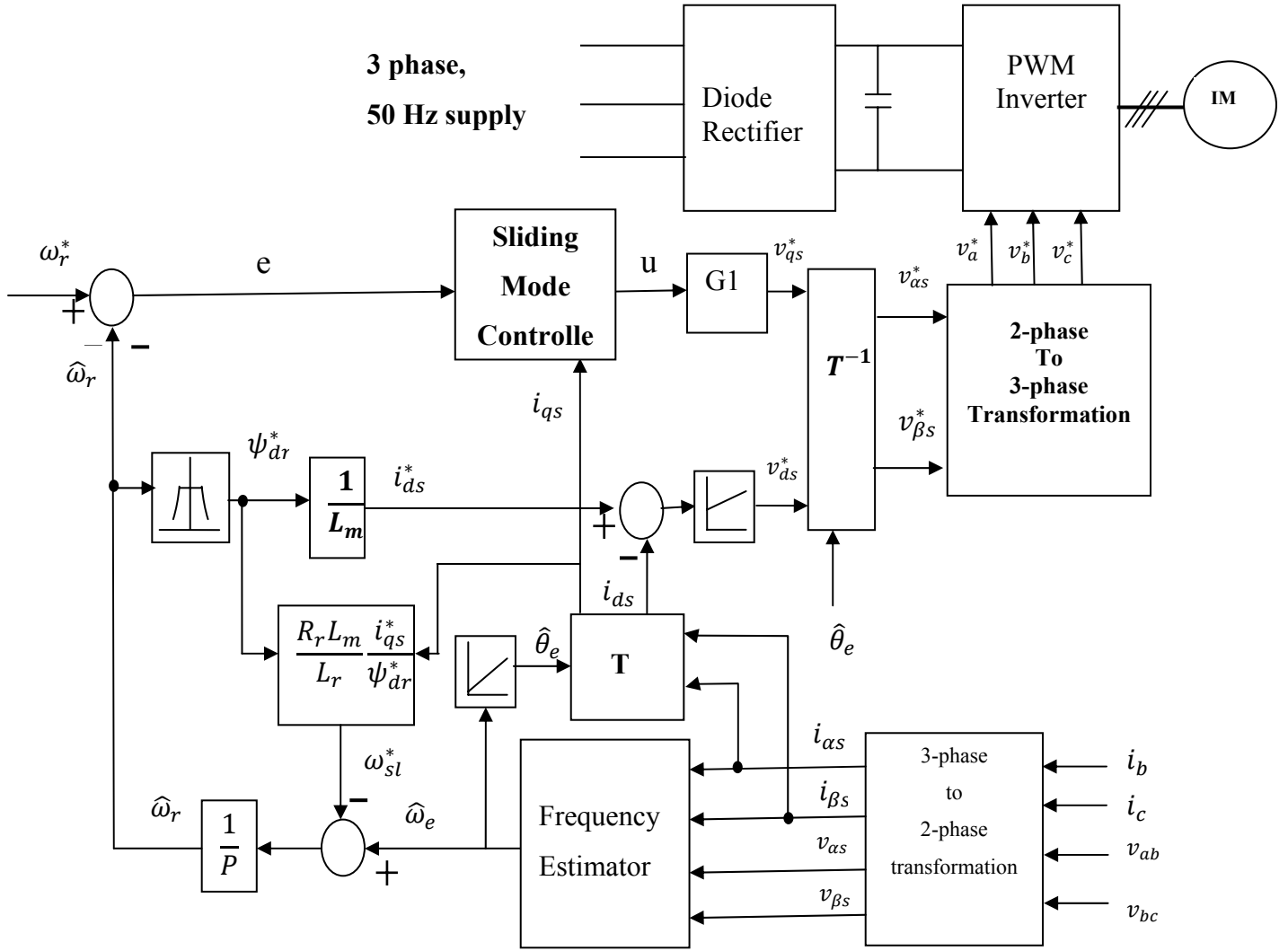


Fig. 3.4 Induction motor drive system with sliding mode controller

3.3 Chapter Conclusion

In this chapter the theory of sliding mode controller is briefly reviewed. The equations in the induction motor model are reorganized so as to apply the control technique. The controller gain and bandwidth are designed, considering various factors such as rotor resistance variations, model inaccuracies, load torque disturbance, to have ideal speed tracking. In the next chapter the simulation results are presented and discussed to validate the proposed control scheme.

Chapter – 4

SIMULATION RESULTS AND DISCUSSIONS

The induction motor drive system is simulated with (i) P-I controller and (ii) sliding mode controller in the mechanical subsystem. Both the controllers are tested for speed tracking and load torque variation conditions. Results are compared among both types of controllers. The drive is subjected to load disturbance to test the robustness of the sliding mode controller.

The rating and parameters of a 3-phase induction motor drive system are given in Appendix –A.

Different cases under which the simulation tests are carried out are:

- (a) Step change in reference speed.
- (b) Tracking of reference speed in trapezoidal form.
- (c) Robustness test against load torque variation.

The comparative study of the results with P-I and SMC are shown bellow.

(a) Step change in reference speed

The reference speed is changed from 1000 rpm to 1200 rpm at time, $t = 1$ sec, and again 1200 rpm to 1500rpm at time, $t = 3$ sec. The reference d-axis rotor flux linkage is kept at 0.45 V.sec and load torque is kept at zero. The simulation responses of the drive system with P-I controller are shown in Fig. 4.1, Fig. 4.2 and Fig. 4.3 and those with sliding mode controller are shown in Fig. 4.4, Fig 4.5 and Fig. 4.6. The responses of speed, speed error, d- and q-axis stator currents, stator phase current (i_a), the control voltage ('u' in SMC) and q-axis stator input voltage (V_{qs}) are shown.

From the figures it is clear that in case of sliding mode controller, the speed error of the system comes to zero faster than fixed gain controller. The q-axis input voltage at the time of transition from one level to another is nearly 20times larger in case of sliding mode controller

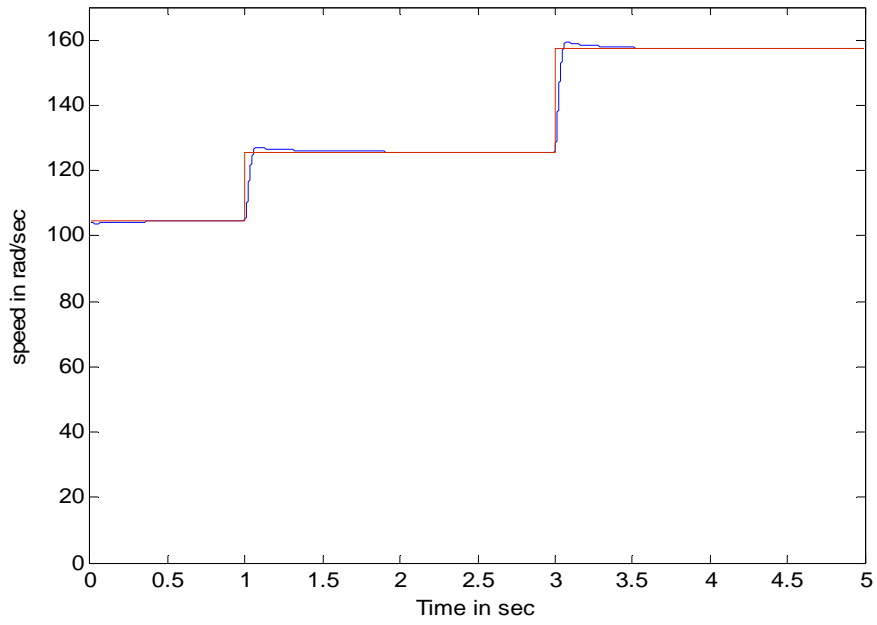
than P-I controller. Similarly the q-axis stator current is much larger in case of sliding mode controller than P-I controller.

(b) Tracking of reference speed in trapezoidal form.

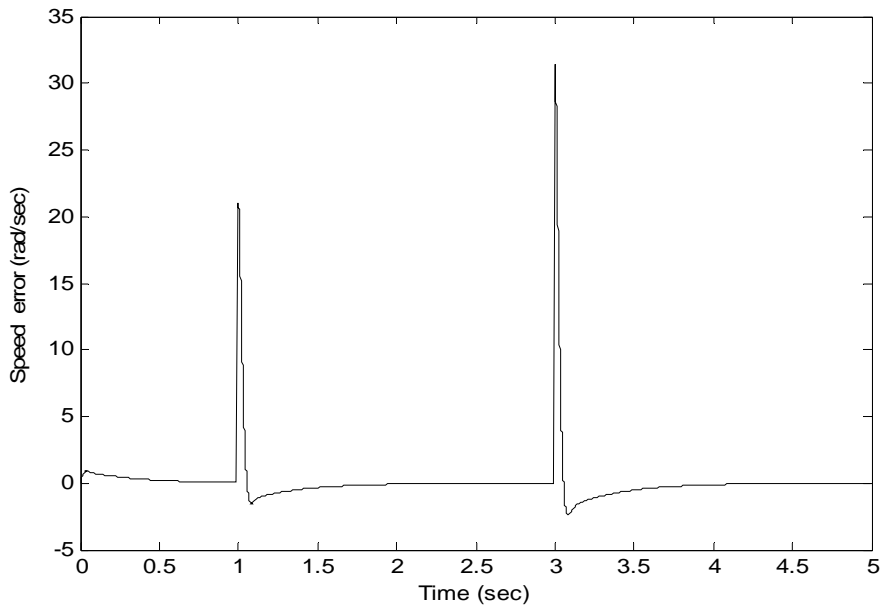
A periodic trapezoidal reference speed is used here to study the tracking performance of the drive system. It is shown in Fig. 4.7 and Fig. 4.8 for fixed gain P-I controller and Fig. 4.9, Fig. 4.10 and Fig. 4.11 for sliding mode controller. The command speed is increased linearly from 0 at $t = 0.6$ sec to 157rad/sec at $t = 1.1$ sec. It is kept constant at 157rad/sec till $t = 2.6$ sec, and decreased linearly to -157rad/sec at $t = 3.6$ sec. Then command speed is kept constant at -157rad/sec till $t = 5.1\text{sec}$ and increased linearly to zero at $t = 5.6$ sec. Same trajectory is used to study the performance of fixed gain P-I controller and sliding mode controller, and results are compared.

Compared to P-I controller the speed tracking performance of sliding mode controller is much better. For both the cases, the q-axis stator voltage, d-and q-axis stator current are shown in the figure. For the sliding mode controller the control input is also shown in the figure.

Fig. 4.12 shows the responses of the controllers during variation of load torque. It is clear that the P-I controller speed response is affected by the load disturbance, where as the sliding mode controller has proved its robustness against load variations.



(a)

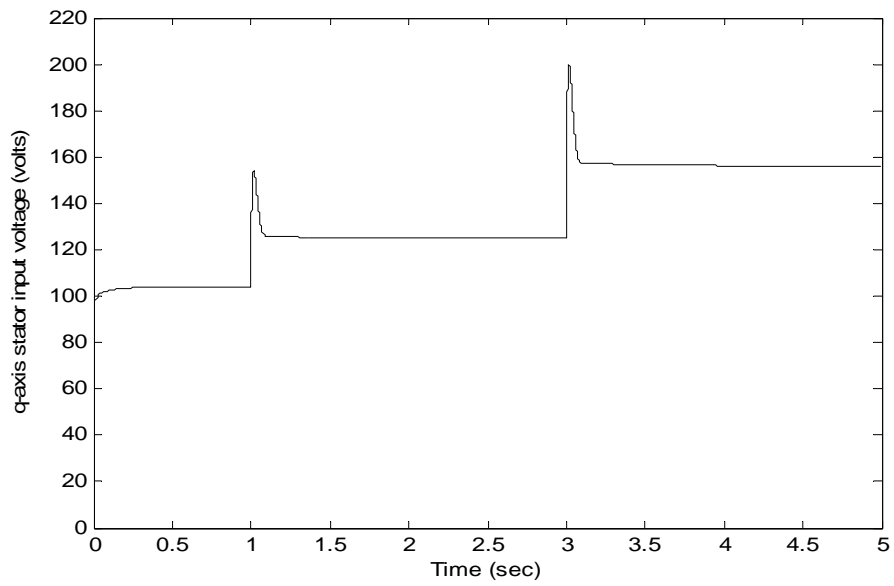


(b)

Fig. 4.1 Step change in reference speed with P-I controller

(a) Speed ,

(b) Speed error,



(a)

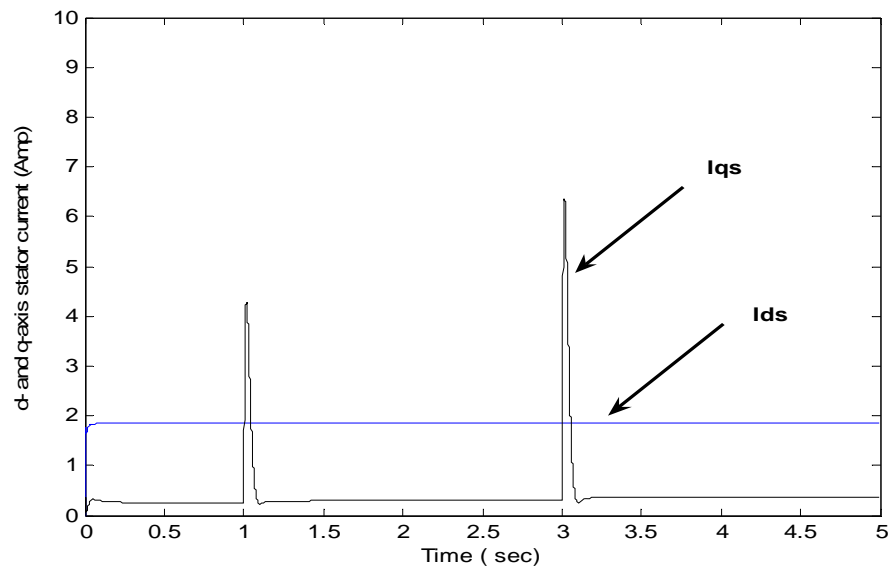


Fig. 4.2 Step change in reference speed with P-I controller

(a) q- axis stator input voltage

(b) d- and q-axis stator current

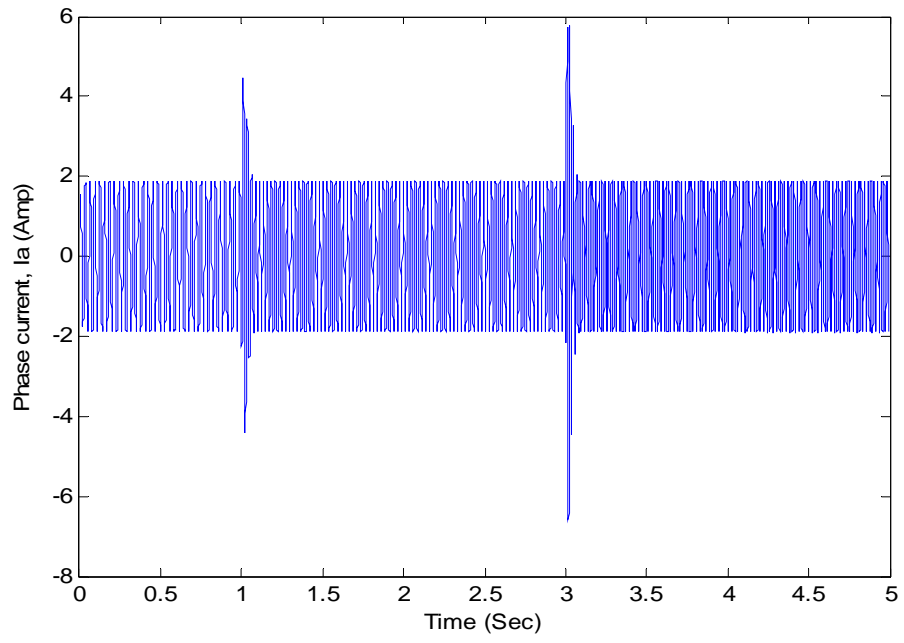
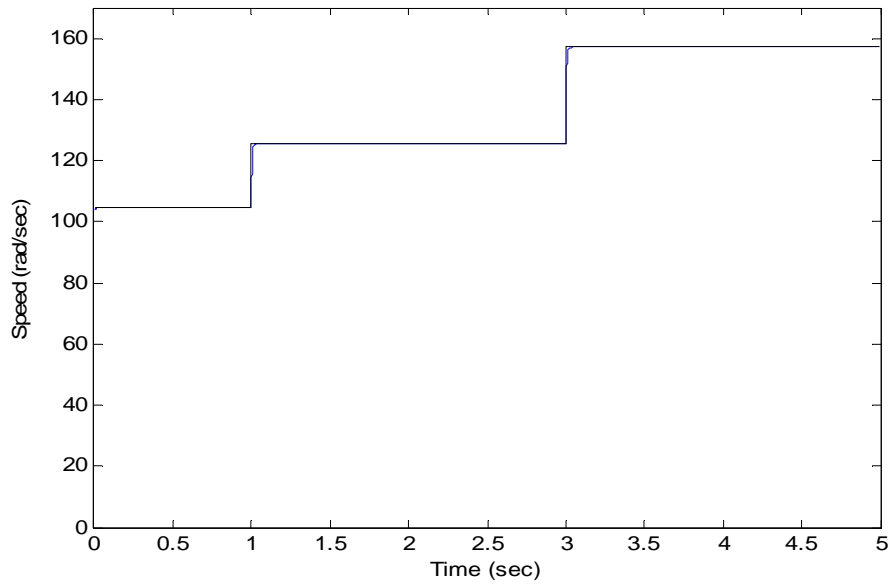
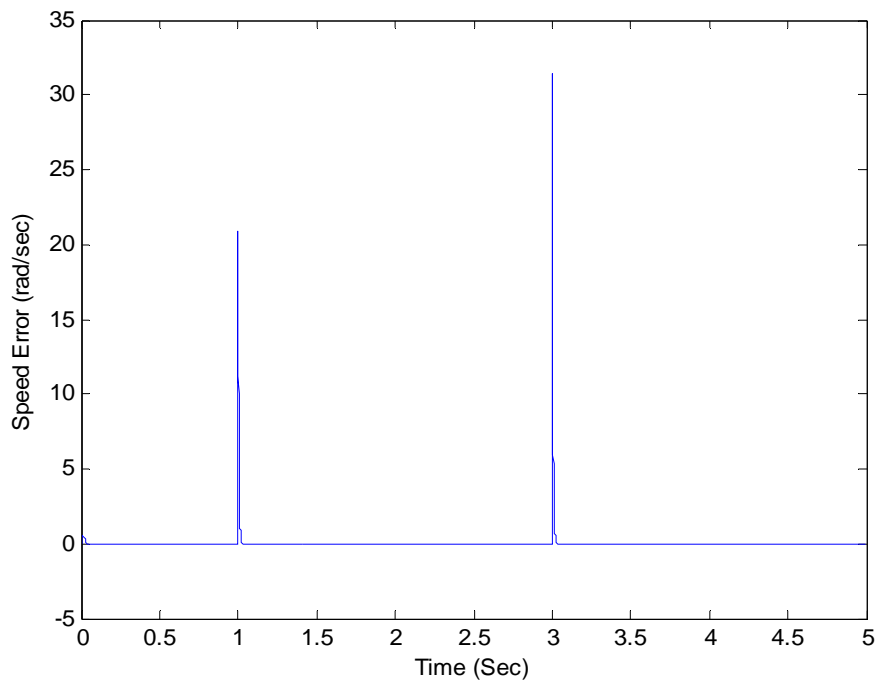


Fig. 4.3 stator phase current (I_a) for step change in reference speed with P-I controller



(a)

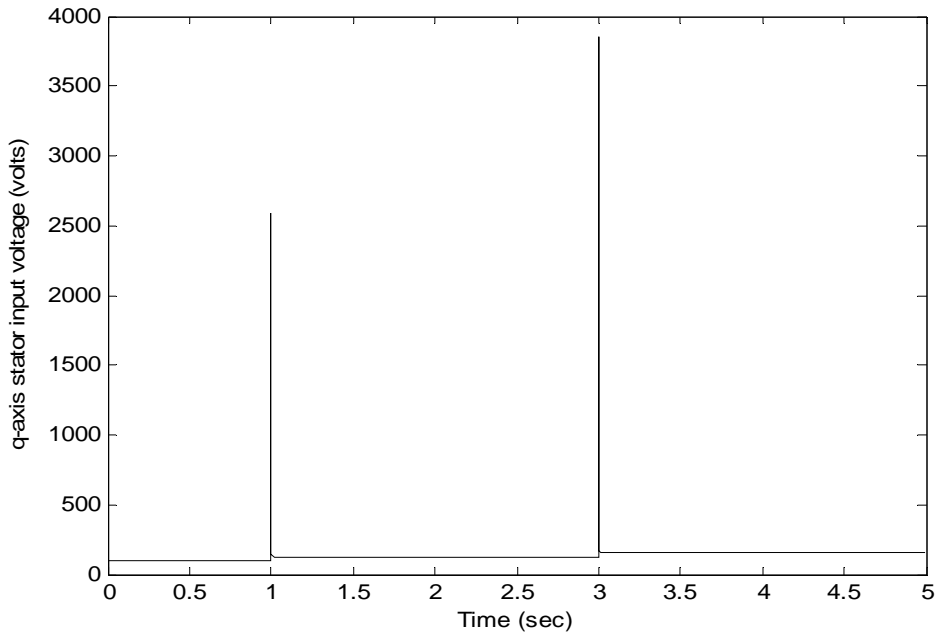


(b)

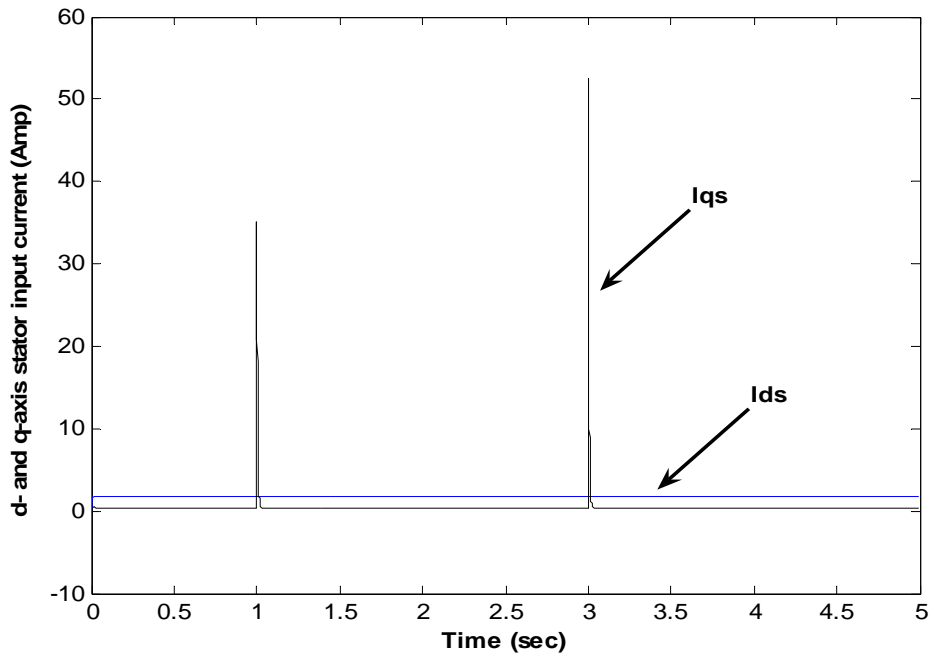
Fig. 4.4 Step change in reference speed with sliding Mode controller

(a) Speed ,

(b) Speed error,



(a)

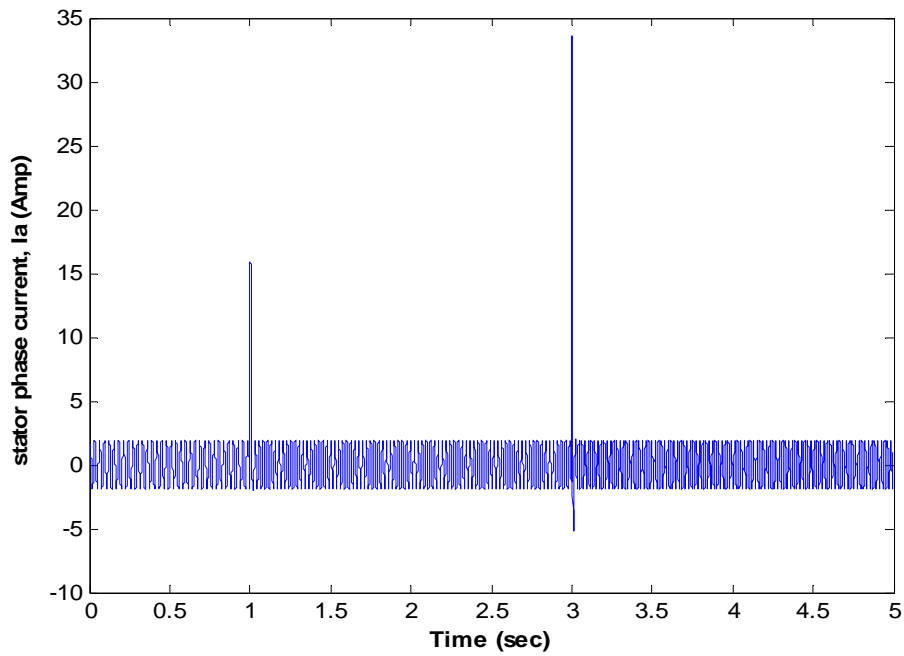


(b)

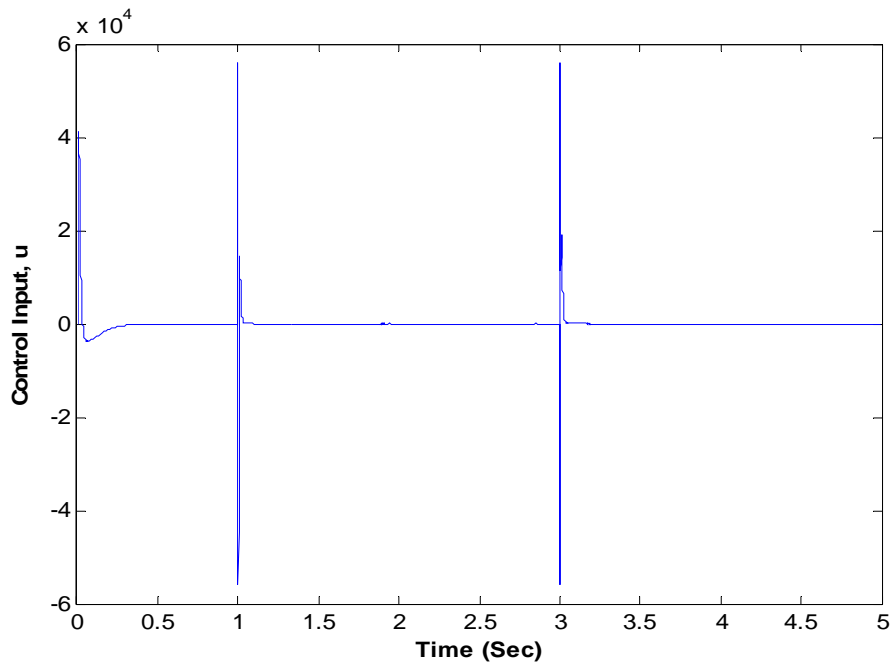
Fig. 4.5 Step change in reference speed with sliding mode controller

(a) q- axis stator input voltage

(b) d- and q-axis stator current



(a)

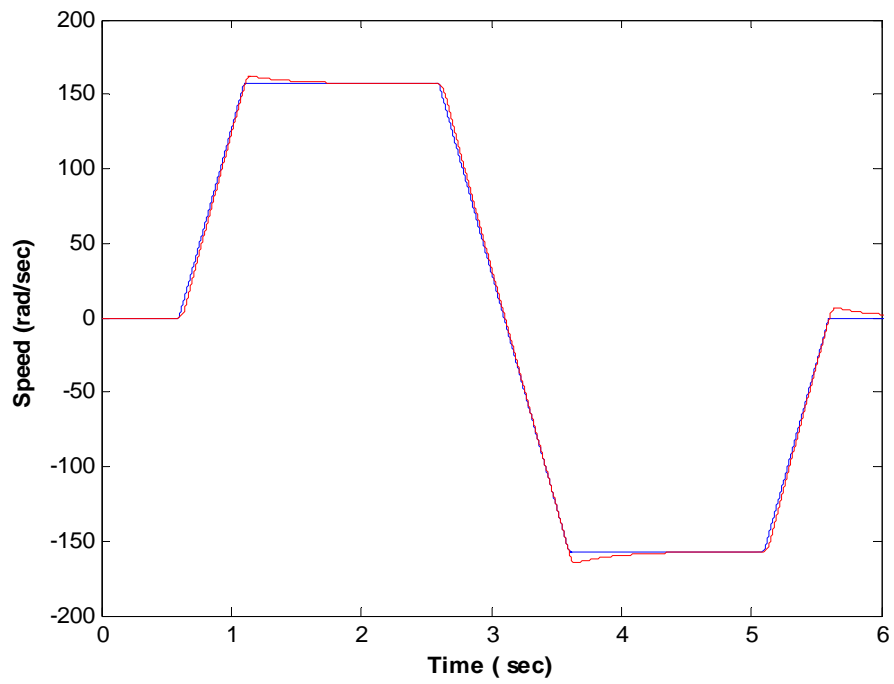


(b)

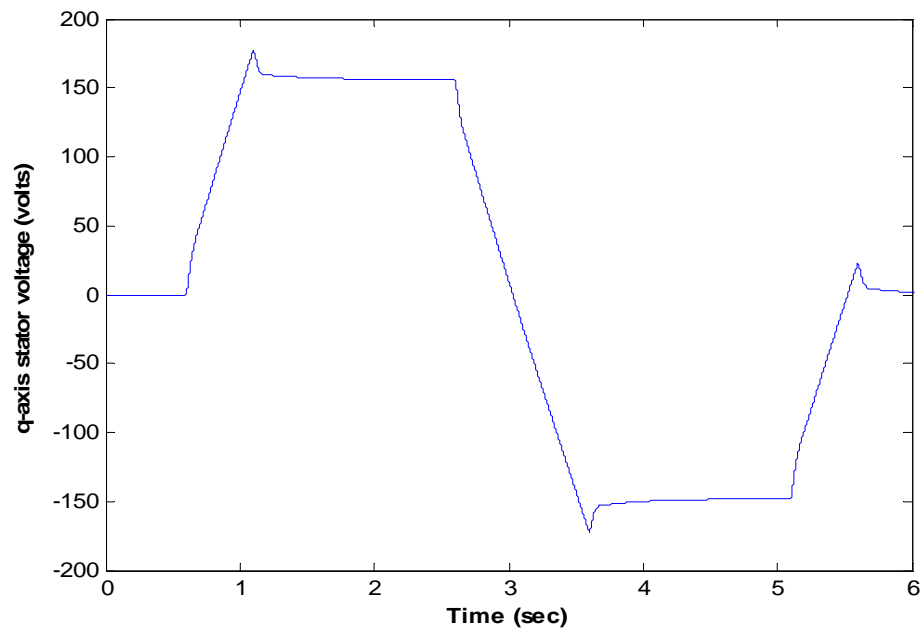
Fig. 4.6 Step change in reference speed with sliding Mode controller

(a) Stator phase current in Amp

(b) Control input, u in rad/s^3



(a)

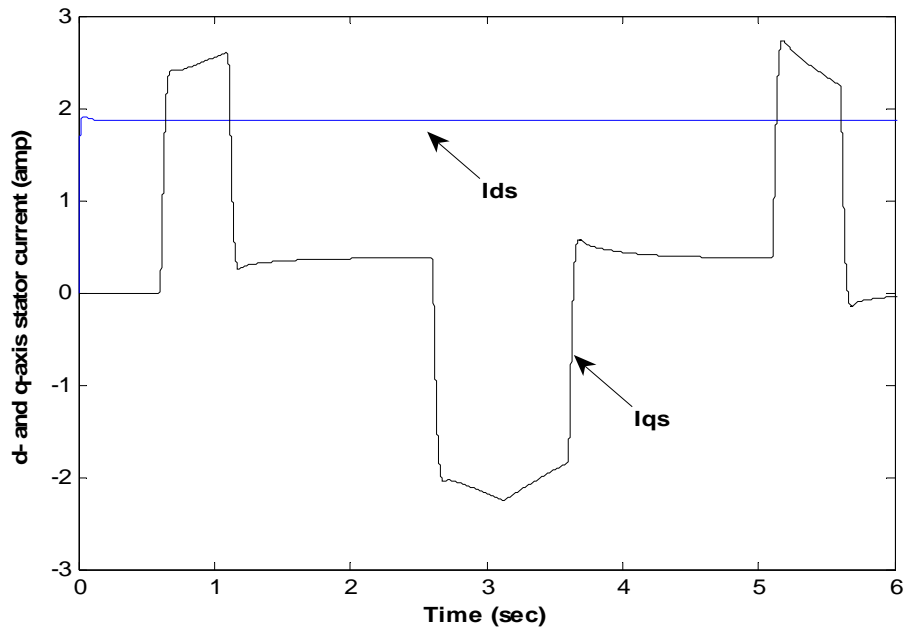


(b)

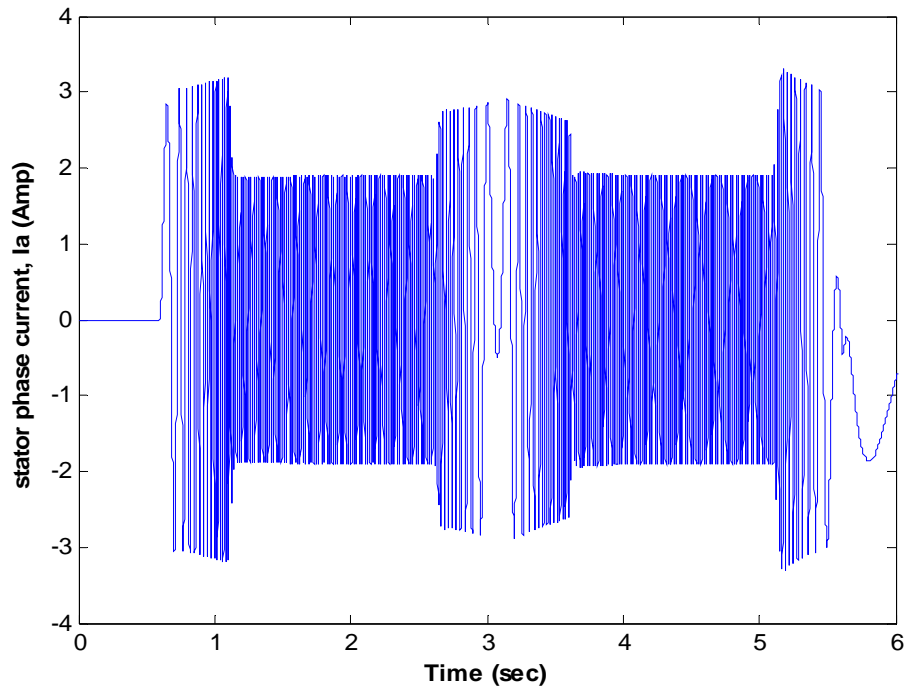
Fig. 4.7 Trapezoidal speed tracking with P-I controller

(a) Speed response

(b) q-axis stator voltage



(a)

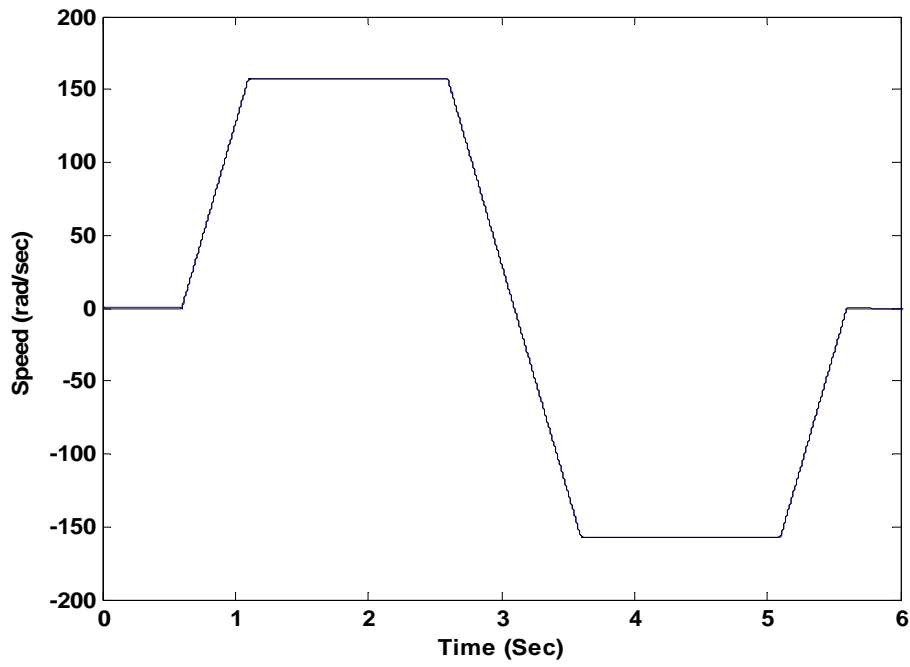


(b)

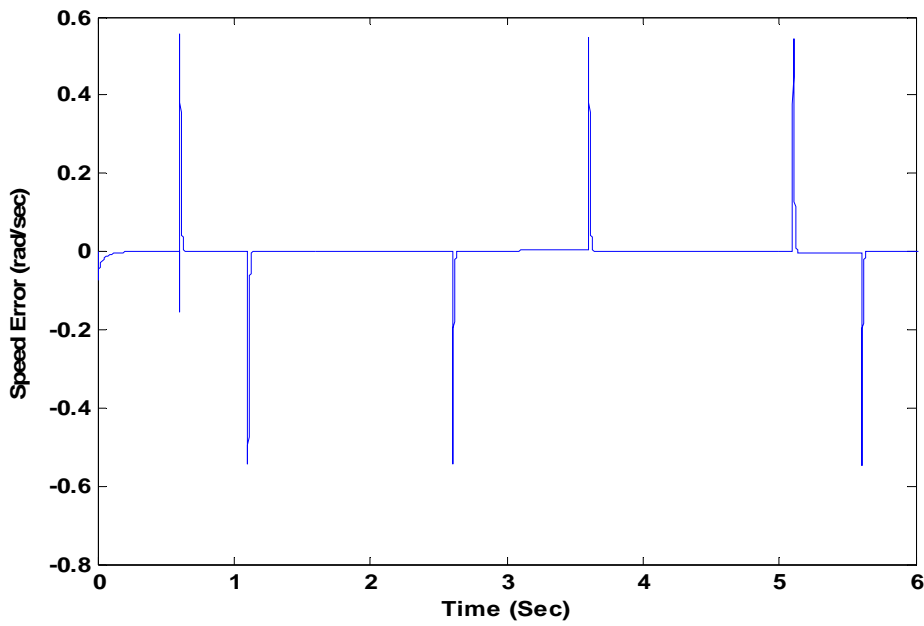
Fig. 4.8 Trapezoidal speed tracking with P-I controller

(a) d- and q-axis stator current

(b) stator phase current



(a)

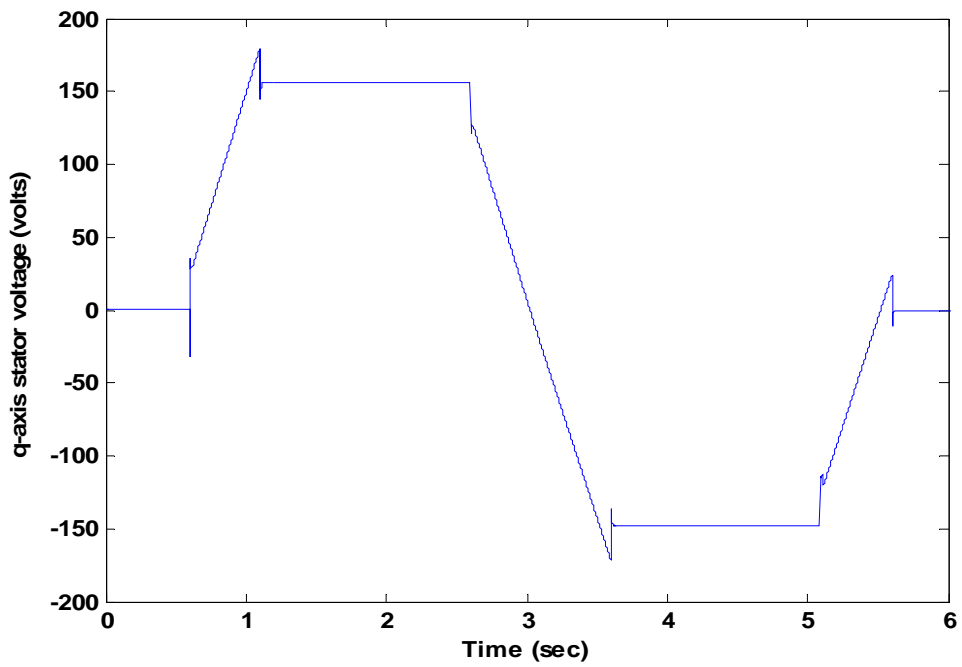


(b)

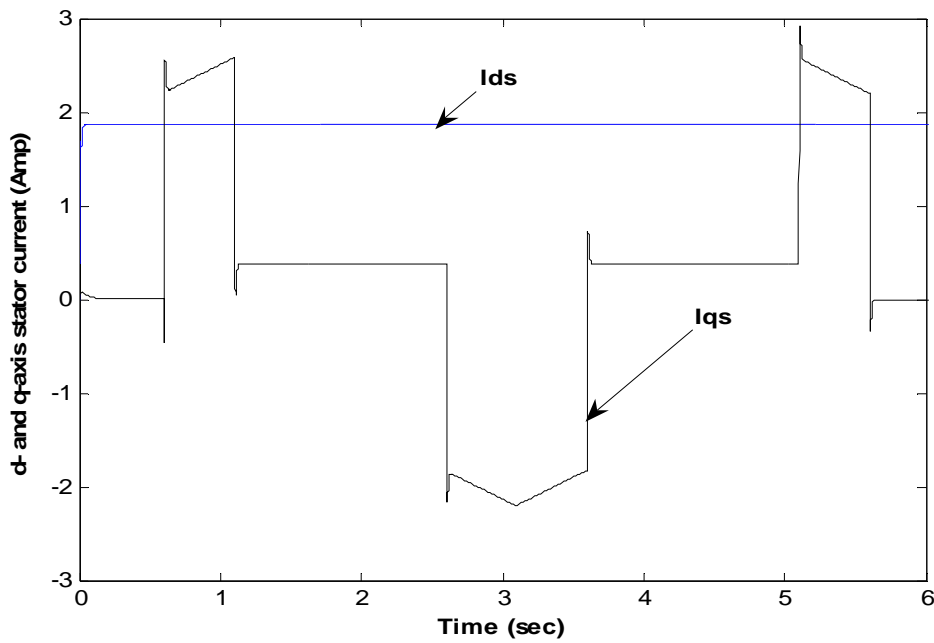
Fig. 4.9 Trapezoidal speed tracking with sliding mode controller

(a) Speed response

(b) Speed Error



(a)

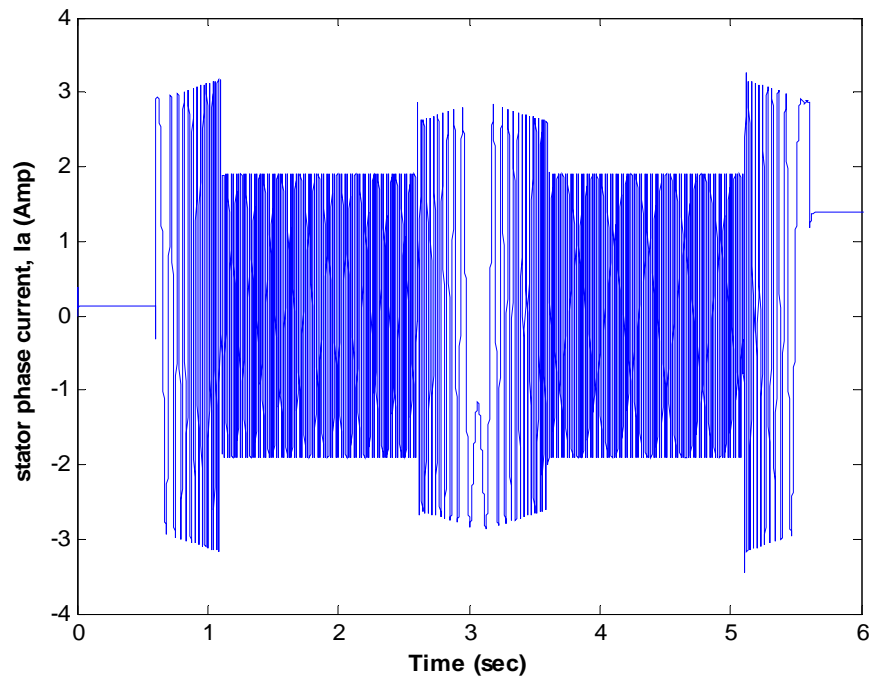


(b)

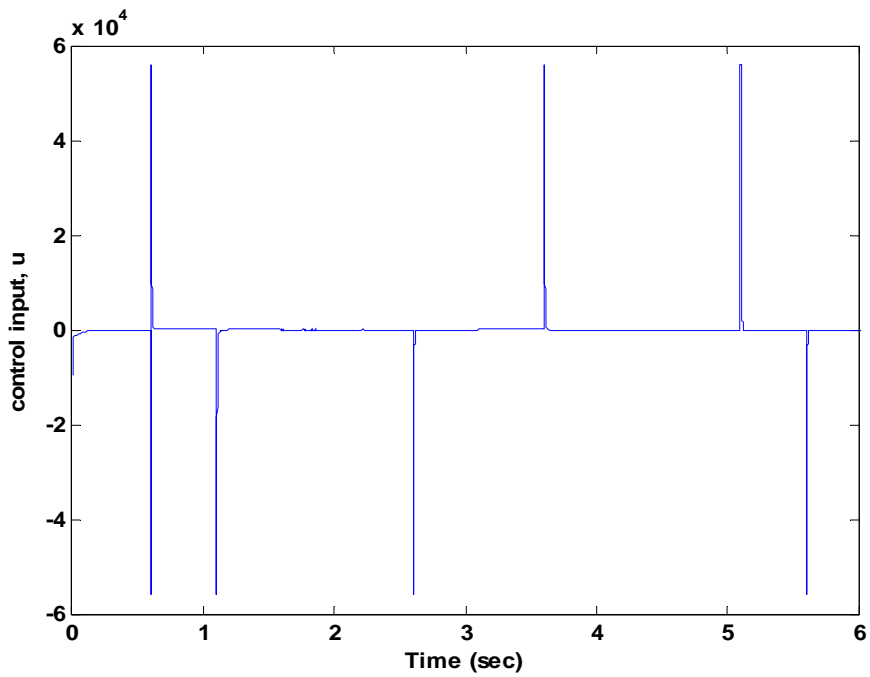
Fig. 4.10 Trapezoidal speed tracking with sliding mode controller

(a) q-axis stator voltage

(b) d- and q-axis stator current



(a)

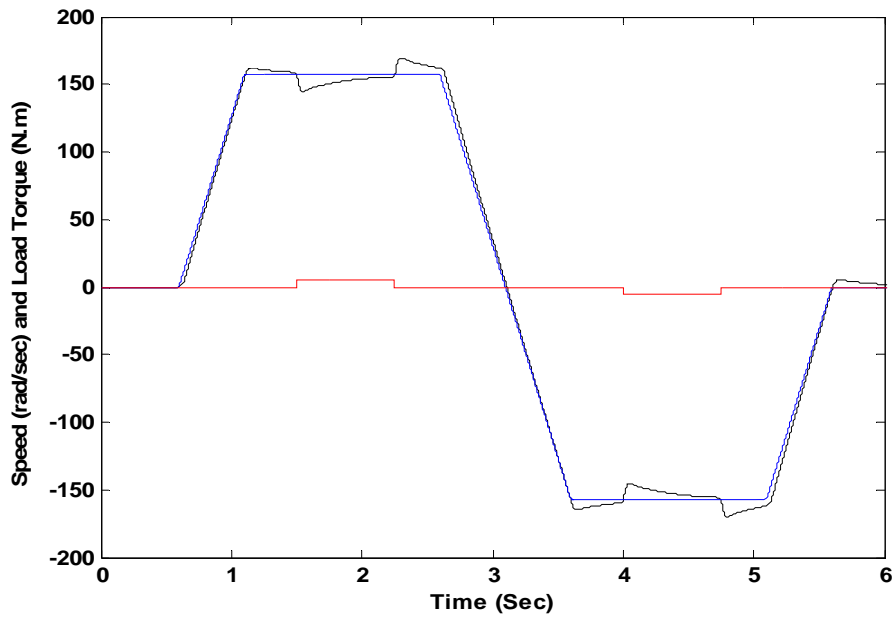


(b)

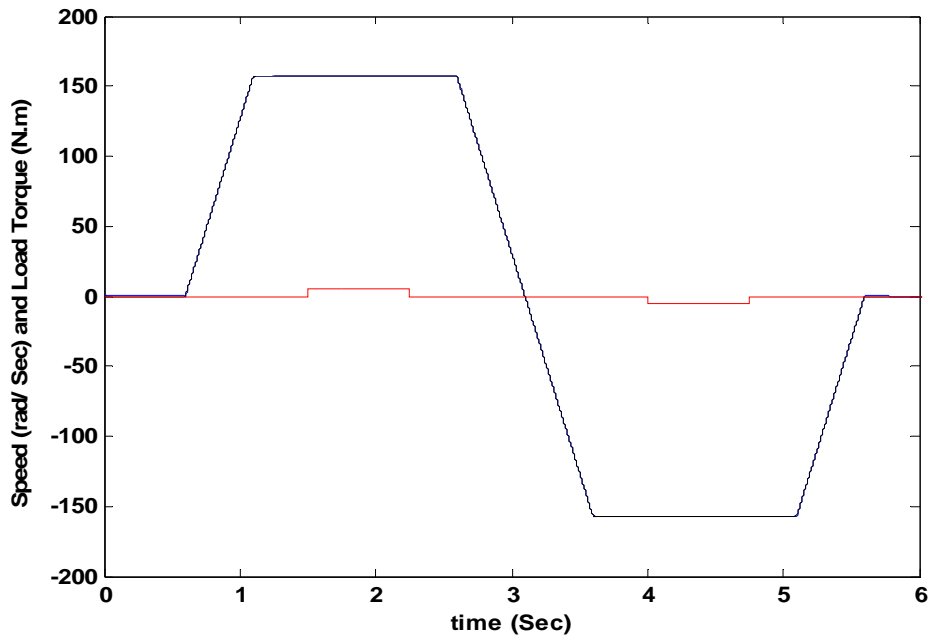
Fig. 4.11 Trapezoidal speed tracking with sliding mode controller

(a) Stator phase current

(b) Control input, u



(a)



(b)

Fig: 4.12 Performance of the drive system under load torque variation

(a) With P-I controller

(b) With Sliding Mode controller

Chapter- 5

CONCLUSION AND FUTURE WORK

In this thesis the theory of sliding mode controller is studied in detail. The equations of the induction motor model are reorganized so as to apply the control technique. The controller gain and band width are designed, considering various factors such as rotor resistance variation, model in accuracies, load torque disturbance and also to have an ideal speed tracking. Considering the case such as load disturbance, the response of the designed sliding mode controller is satisfactory. It also gives good trajectory tracking performance. The speed regulation characteristic is also satisfactory.

Only load disturbance is the problem considered in this case and the robustness of the controller is verified. Since the machine rating is small, the resistance variation effect is very small. Hence has negligible effect. As a future work this controller can be applied to any other drive system with higher rating where parameter variation effect can be studied. Fuzzy logic Principle can be incorporated to this controller to make it more efficient and robust.

REFERENCES

- [1] Bose B.K., "Modern Power Electronics and AC Drives", *Pearson Education, 4th Edition, 2004*
- [2] R.M. Cuzner, R.D. Lorenz, D.W. Novotny, "Application of non-linear observers for rotor position detection on an induction motor using machine voltages and currents," IEEE-IAS Annual Meeting Conference Record, October 1990, pp. 416–421.
- [3] Atkinson D. J., P. P. Acarnley and J. W. Finch, "Application of estimation technique in vector controlled inductin motor drives," IEE Conference Proceeding, London, July 1990, pp. 358-363.
- [4] A. Ferrah, K.G. Bradely, G.M. Asher, "Sensorless speed detection of inverter fed induction motors using rotor slot harmonics and fast Fourier transform," IEEE-PESC Conference Record, October 1992, pp. 279–286.
- [5] Baader U., M. Depenbrock, and G. Gierse, "Direct self control of inverter- fed induction machines: A basis for speed control without a speed measurement," IEEE Trans. Ind. Appl., vol. 28, no. 3, May 1992, pp. 581-588.
- [6] Blaschke F., " The principle of field orientation as applied to the new TRANSVECTOR closed loop control system for rotating field machines," Siemens Review, vol. 93, no. 5, may 1970, pp. 217-220.
- [7] Chan, C. C., and H. Q. Wang, "New scheme of sliding mode control for high performance induction motor drives," IEE Proc. on Electric Power Applications, vol. 143, no. 3, May 1996, pp 177- 185.
- [8] Chan C. C., Leung W. S. and C. W. Nag, " Adaptive decoupling control of induction motor drives," IEEE Transaction on Industrial Electronics, vol. 35, no. 1, Feb. 1990, pp.41-47.
- [9] N. Teske, G.M. Asher, M. Sumner, K.J. Bradely, "Suppression of saturation saliency effects for the sensorless position control of induction motor drives under loaded conditions," IEEE Trans. Ind. Appl. 47 (5) (2000) 1142–1150.

- [10] N. Teske, G.M. Asher, M. Sumner, K.J. Bradely, Encoderless position estimation for symmetric cage induction machines under loaded conditions, *IEEE Trans. Ind. Appl.* 37 (6) (2001) 1793–1800.
- [11] Dunningan, M. W., S. Wade, B. W. Williams, and X. Xu, “Position control of a vector controlled induction machine using Slotine’s sliding mode control approach,” *IEE Proc. on Elect. Power Appl.*, vol. 145, no. 3, May 1998, pp. 231- 238.
- [12] Garces L. J., “Parameter adaptation for speed controlled static AC drives with a squirrel cage induction motor,” *IEEE Trans. On Industry Applications*, vol. 16, no. 12, Mar. 1980, pp 173 -178.
- [13] Hasse K., “ On the dynamic behavior of induction machines driven by variable frequency and voltage sources,” *ETZ Arch. Bd.* 89, H. 4, 1968, pp. 77-81.
- [14] Hung K. T., and R. D. Lorenz, “ A rotor flux error based adaptive tuning approach for feed forward field oriented induction machine drives,” *IEEE Conf. record IAS annual meeting*, 1990, pp. 594-598.
- [15] Kim Y. R., S. K. Sul and M.H. Park, “ Speed sensorless vector control of induction motor using extended Kalman filter,” *IEEE Transaction on Ind. Appl.*, Vol. 30, no. 5, 1994, pp. 1225-1233.
- [16] Krause P. C., *Analysis of Electric Machinery*, McGraw-Hill, New York, 1986
- [17] Krause P. C and C. S. Thomas, “Simulation of symmetrical induction machinery,” *IEEE Trans. on Power Apparatus & Systems*, vol. 84, no. 11, 1965, pp. 1038- 1053.
- [18] Krishnan R. and A. S. Bharadwaj, “ A review of parameter sensitivity and parameter deviations in feed forward field oriented drive systems,” *IEEE Transaction on power Electronics*, vol.6, no. 4, 1991, pp. 695- 703.
- [19] Mohanty K. B., A. Routray and N. K. De, “Rotor flux oriented sensor less induction motor drive for low power applications.” *Proceeding of Int. Conference on Computer Application in Electrical Engg.: Recent Advances (CEERA)*, Feb, 2001, Roorkee, pp. 747- 752
- [20] Nilsen R. and M. P. Kazmeirkowski, “ Reduced order observer with parameter adaptation for fast rotor flux estimation in induction machin,” *IEE Proceeding*, vol. 136, no. 1, Jan. 1989, pp. 35-43.

- [21] Park, T. G., and K. S. Lee, "SMC based adaptive input-output linearizing control of induction motors," IEE Proc. on Control Theory Applications, vol. 145, no. 1, Jan 1998, pp. 55-62.
- [22] Rajsekhar K., A. Kawamura, and K. Matsuse, "*Sensorless control of AC motor drives: Speed and Position sensorless operation*," Piscataway, NJ, IEEE press, 1996.
- [23] Soto, R., and K. S. Yeung, " Sliding mode control of induction motor without flux measurement," IEEE Transaction on Industrial Application, vol. 31, no. 4, 1995, pp.744-751.
- [24] Tajima H. and Y. Hori, " Speed sensorless field oriented control of induction machine," IEEE Transaction on Industrial Application, vol. 29, no. 1, 1993, pp.1003-1008
- [25] Utikin, V. I., " Variable structure system with sliding mode: A Survey," IEEE Transaction on Automatic control, vol. 22, no, 2, 1977, pp. 212-222
- [27] Zhen L., and L. Xu, " sensorless field orientation control of induction machines based on a mutual MRAS scheme," IEEE Transaction on Industrial Electronics, vol.45, no. 5, Oct. 1998, pp824-831.
- [28] Benchaib, A., A. Rachid, and E. Audrezet, " Sliding made input-output linearization and field orientation for real time control of induction motors," IEEE Trans. on Power Electronics, vol. 14, no.1, Jan 1999, pp.128- 138.
- [29] Benchaib, A., A. Rachid, E. Audrezet, and M. Tadjine, "Real time sliding mode observer and control of an induction motor," IEEE Trans. on Ind. Electronics, vol. 46, no. 1, Feb 1999, pp. 128-138.
- [30] Mohanty K.B., "Sensorless sliding mode control of induction motor drives," TENCON-2008, IEEE Region 10 Conference, Hyderabad.
- [31] A. Derdiyok, M. K.Guven, Habib-Ur Rahman and N. Inane, "Design and Implementation of New Sliding-Mode Observer for Speed- Sensorless Control of Induction Machine," IEEE trans. on Industrial Electronics, Vol. 1, No.3, 2002.
- [32] Barambones, O. and Ggarrido, A.J, "A sensorless variable structure control of induction motor drives," Electric Power systems Research, 2004, pp 21-32

APPENDIX- A

Parameters of Typical Induction Machine

Three phase, 50 Hz, 0.75kW, 220V, 3A, 1440rpm

Stator Resistance $R_s = 6.37\Omega$

Rotor resistance $R_r = 4.3\Omega$

Stator inductance $L_s = 0.26H$

Rotor Inductance $L_r = 0.26H$

Mutual Inductance $L_m = 0.24 H$

Number of Poles $P = 4$

Moment of inertia of motor and load $J = 0.0088\text{Kg.m}^2$

Viscous friction coefficient $B = 0.003 \text{ N.m.s/rad}$

Proportional cum Integral controller parameters

Speed loop PI controllers

$K_{p1} = 0.35$ $K_{i1} = 1$

$K_{p2} = 100$ $K_{i2} = 29877$

Flux loop PI controller

$K_{p3} = 151.27$ $K_{i3} = 43649$